Tu-Pos484

WHY MAGAININ PEPTIDES CAN DISCRIMINATE BETWEEN BACTERIAL AND ERYTHROCYTE MEMBRANES?

((K. Matsuzaki, K. Sugishita, N. Fujii and K. Miyajima)) Fac. Pharm. Sci., Kyoto University, Sakyo-ku, Kyoto 606-01, JAPAN

Magainins (MGs), a class of antimicrobial peptide isolated from *Xenopus* skin, permeabilize bacterial membranes. However, they are practically nonhemolytic. Both membrane systems greatly differ in lipid composition. Thus, we examined the effects of lipid composition on the lytic activity of MG 2 and compared them with those of melittin (ML), a lytic peptide. The lytic power of MG 2 to liposomes of phosphatidylglycerol, abundant in bacterial membranes, was ten times stronger than that of ML. In contrast, the MG2-induced permeabilization of bilayers of phosphatidylcholine, mainly localized in the outer half of the erythrocyte membrane was two orders of magnitude weaker than that by ML, in keeping with MG's much weaker hemolytic activity. The formation of phosphatidic acid on erythrocyte surface by a phospholipase D treatment enhanced the peptide binding to and the lysis of erythrocytes. The incorporation of cholesterol, rich in the erythrocyte membrane, reduced the lysis by MG 2. The application of a transmembrane potential enhanced MG's hemolytic activity. We can conclude that the absence of any acidic lipids on the outer monolayer and the abundant presence of cholesterol, combined with the lack of a transmembrane potential, protect erythrocytes from MG's attack.

Tu-Pos485

ELECTRO-ELASTIC COUPLING IN MODELING IONIC TRANSPORT DYNAMICS IN TRANSMEMBRANE ION CHANNELS.

((M.B. Partenskii and P.C. Jordan)) Dept. of Chemistry, Brandeis University, Waltham, MA 02254.

General analysis and a specific illustration using an exactly soluble "elastic capacitor" model have shown (Partenskii and Jordan, *J.Chem.Phys.* **99**:2992 [1993]) that coupling between quasielastic (of interactive and/or entropic origin) and electrical degrees of freedom can cause such peculiarities at electrified interfaces as a negative branch of differential capacity, multistability and related electrical instabilities and phase transitions. The same mechanism may well have significant impact on the evolution of ionic current through an ion channel. Coupling of a charging process, induced by a transmembrane voltage, with structural changes in the channel (local deformation, bond libration, water dipole alignment, etc.) is described by switching the elastic capacitor in parallel with the pore's internal resistance, $R_{int}(x)$; x is the "gap width" of the capacitor (introduced to model voltage induced structural deformation in the pore-protein system). External resistance R_{ext} accounts for ionic diffusion from the solvent to the channel mouth. The other model parameters are an effective friction, affecting the time evolution of the elastic system, and the applied voltage, V. Analysis of the resulting nonlinear differential equations demonstrates self-oscillation of charge, current and elastic deformation for a range of model parameters. The possible interrelation between this effect and j(t) behavior of single ion channels is discussed.

MOLECULAR MECHANISMS OF MECHANOTRANSDUCTION: FROM BACTERIA TO BUCKMINSTER

W-AM-SymI-1

MECHANOSENSITIVE ION CHANNELS IN THE *E. COLI* CELL ENVELOPE: FROM PATCH-CLAMP STUDIES TO MOLECULAR IDENTIFICATION.

((B. Martinac[1], A.H. Delcour[2], M. Buechner[3], S.I. Sukharev[4], P. Blount[4], J. Adler[5] and C. Kung[4,6])) Dept Pharmacol[1], Univ of Western Australia, Perth, WA, Australia; Dept Biol[2], Univ of Houston, Houston, TX, USA; Dept Biol[3], Johns Hopkins University, Baltimore, MD, USA; Lab Mol Biol[4], Dept Biochem[5] and Dept Genetics[6], Univ of Wisconsin, Madison, WI, USA.

We used the patch-clamp technique to study the mechanosensitive ion channels (MSCs) of *Escherichia coli* in various experimentally-induced giant forms, and also in reconstituted bacterial membrane fractions. The membrane envelope of giant spheroplasts of *E. coli* exhibits activities of two distinct types of MSCs, the small MSC (MscS) and the large MSC (MscL) with conductances of approximately 1 and 3 nS (in 200 mM KCl) respectively. The effects of lysozyme and various amphipathic compounds on the activity of the MscS in membrane patches of giant spheroplasts indicated that (i) the peptidoglycan (cell wall) acted to resist the membrane stretching, and (ii) the lipid bilayer alone could transduce the mechanical force along the membrane plane which opened the channel. Both the MscS and the MscL can be functionally reconstituted into azolectin liposomes, either by fusing native membrane vesicles or by reassembly of the octylglucoside-solubilized membrane extract. This result strongly supported the previous findings that both types of channels are gated by tension transduced via the lipid bilayer. The nonselective MscL activated by high negative pressures and the weakly anion-selective MscS activated by lower negative pressures applied to a patch-clamp pipette appeared more sensitive to suction in liposomes than in spheroplasts. This finding suggested further that the cell wall restrains the membrane stretch. With detergent solubilization of the cell envelope followed by gel filtration of the solubilized membrane extract and patch-clamp sampling of individual fractions reconstituted into liposomes, we demonstrated that the MscL and the MscS are distinct proteins under nondenaturing conditions with approximate m.w. of 60-80 kD and 200-400 kD repectively. In addition, with SDS-PAGE we were able to trace the MscL to a small protein of approximately 17 kD. This protein was electroblotted and microsequenced. The sequence of 37 N-terminal amino-acid residues was found to correspond to a protein of previously unknown function encoded by a gene we have named *mscL* on a genomic fragment at minute 72 of the *E. coli* chromosome. Since insertional disruption of *mscL* removed the channel activity and re-expression of *mscL* carried on an expression plasmid restored its activity, we conclude that the *mscL* gene encodes a protein responsible for the activity of the MscL in *E. coli*.

W-AM-SymI-2

TOUCH INSENSITIVE MUTANTS IN *C. ELEGANS*.

((M. Driscoll)) Dept. of Molecular Biology and Biochemistry, Rutgers University, Center for Advanced Biotechnology and Medicine, 679 Hoes Lane, Piscataway, NJ 08855.

Mechanosensation in the nematode *Caenorhabditis elegans* is mediated by six mechanosensory neurons called touch receptor cells. M. Chalfie and colleagues have identified over 400 mutations that disrupt the function of the touch receptors (*Science* 243:1027 (1989)). These mutations define 15 *mec* genes (so named because elimination of their activity renders animals *mec*hanosensory defective) specifically required for the development and function of the touch receptor neurons. Some of these genes are expected to encode products directly involved in mechanotransduction.

mec-4 encodes a subunit of a newly discovered type of ion channel that is a candidate mechanosensory channel. *mec-4* is also of considerable interest because specific amino acid changes in the MEC-4 protein can induce the degenerative death of the touch receptor neurons. Our structure/function analysis of the MEC-4 protein has highlighted the functional importance of charged and polar amino acid residues which align on one face of the predicted α helix thought to form the second membrane-spanning domain, MSDII. We speculate that MSDII lines the channel pore and that essential amino acids project into the channel lumen to influence ion transport. Other genetic and molecular studies are consistent with a model in which the mechanosensory channel is a multimer that includes more than one MEC-4 subunit and a subunit homologous to MEC-4. We are beginning to test this detailed model of channel structure using biochemical and electrophysiological approaches. Consistent with the claim that mechanosensory channels are ubiquitous, *mec-4* is a member of a rapidly growing family of identified genes from *C. elegans* and higher organisms that appear to be expressed in diverse cell types.

W-AM-SymI-3

PRESSURE-CLAMP MEASUREMENTS OF THE DYNAMIC PROPERTIES OF MECHANO-GATED CHANNELS.

((O.P. Hamill and D.W. McBride, Jr.)) Department of Physiology and Biophysics, UTMB, Galveston, TX 77555.

Mechano-electrical transduction (MET) is typically associated with a generator potential that arises through an increase in membrane conductance to cations (Na^+, K^+ and Ca^{++}). Patch-clamp characterization of a stretch-activated cation channel in skeletal muscle fibers (Guharay & Sachs, J. Physiol, 352:685,1984) demonstrated that mechanical stimulation affected channel gating rather than channel conductance. Subsequently, the development of a pressure-clamp technique (McBride & Hamill, Pflugers. Archiv. 421:606, 1992) has revealed dynamic properties of mechano-gated (MG) channels. Pressure jump analysis of the MG channel in muscle and *Xenopus* oocytes has enabled the characterization of the pressure and voltage dependence of the latency, turn on and turn off kinetics of mechano-gated channels. Adaptation of MG channel activity to sustained stimulation was found in both cell types. In general, adaptation enables mechanotransducers to maintain their dynamic sensitivity over a broad stimulus domain. In nonsensory cells it may also serve to limit Ca^{++} influx. Adaptation of MG channel activity is voltage dependent but occurs in the absence of Ca^{++} (Hamill & McBride, PNAS 89:7462,1992). Mechanical stimulation of the patch can abolish adaptation. This result indicates that membrane-cytoskeleton coupling is important for adaptation.

W-AM-SymI-4

MECHANOELECTRICAL TRANSDUCTION IN THE VERTEBRATE HAIR CELL.

((R.A. Eatock)) Dept. of Otolaryngology, Baylor College of Medicine, Houston, TX 77030.

Hair cells are the mechanoreceptive cells of the lateral line and inner ear. Stimulation deflects the cells' hair bundles: arrays of modified microvilli (stereovilli) that protrude from the apical surfaces. Deflection of the hair bundle modulates channels near the tips of the stereovilli (Jaramillo & Hudspeth, Neuron 7:409, 1991). In the prevailing model of transduction, the channels are gated by elastic elements ("gating springs") that stretch in response to deflections of the hair bundle in one direction and relax during deflections in the opposite direction (Corey & Hudspeth, J. Neurosci. 3:962, 1983). Candidate gating springs, called tip links, have been identified; these are filamentous connections between stereovilli in adjacent rows (Pickles et al., Hearing Res. 15:103, 1984). The transduction process adapts in a calcium-dependent fashion, shifting the operating range in the direction of the stimulus (Eatock et al., J. Neurosci. 7:2821, 1987). One model of adaptation proposes that the gating springs are linked by myosin to the actin cores of the stereovilli and that movement of the myosin along the core restores the gating springs to (near) their resting lengths (Howard & Hudspeth, Proc. Natl. Acad. Sci. 84:3064, 1987; Assad & Corey, J. Neurosci. 12:3291, 1992). An alternative model (Crawford et al., J. Physiol. 419:405, 1989) proposes that calcium ions that enter open transduction channels promote channel closure.

W-AM-SymI-5

MECHANOCHEMICAL TRANSDUCTION ACROSS INTEGRINS AND THROUGH THE CYTOSKELETON ((D. E. Ingber)) Departments of Pathology & Surgery, Children's Hospital, Harvard Medical School, Boston, MA 02115.

We have explored the possibility that the cellular response to force is based upon transfer of mechanical signals across transmembrane receptors (integrins) that mediate cell attachment to extracellular matrix (ECM) and subsequent structural changes in the cytoskeleton. This concept is based on studies with cultured cells which demonstrate that cell shape, growth and function can be controlled by varying the number of ECM attachment sites that physically resist cytoskeletal tension. Recently, we have used a magnetic twisting device in which controlled mechanical stresses are applied directly to cell surface integrin receptors using RGD-coated ferromagnetic microbeads (5.5 μm diameter) and the cytoskeletal response is simultaneously measured using an in-line magnetometer (Wang et al., Science, 1993; 1124-1127). Using this approach, we found that the transmembrane ECM receptor, β_1 integrin, effectively transferred mechanical loads across the cell surface and supported a force-dependent cytoskeletal stiffening response whereas non-adhesion receptors did not. Force transfer correlated with recruitment of focal adhesion proteins and linkage of integrins to the actin cytoskeleton. Yet the cytoskeletal response to stress involved microtubules and intermediate filaments as well as microfilaments. The stiffness of the cytoskeleton also increased in direct proportion as the level of applied stress was raised. This behavior was mimicked using stick and string "tensegrity" models that contain mechanically-interdependent structural elements that rearrange rather than deform locally in response to stress. Tensegrity models also predict how molecular patterns (e.g., actin geodomes, stress fibers) develop within the cytoskeletal lattice in response to changes in the distribution of mechanical stresses. As a result of force-induced cytoskeletal rearrangements, mechanochemical transduction may be mediated simultaneously at multiple locations inside the cell.

SR Ca^{2+} RELEASE CHANNELS II

W-AM-A1

SINGLE CHANNEL PROPERTIES OF THE CLONED EXPRESSED CALCIUM RELEASE CHANNEL (RYANODINE RECEPTOR)
((K. Ondrias, A-M. B. Brillantes, A. Scott, E. Ondriasova, B.E. Ehrlich*, and A.R. Marks)) Mount Sinai School of Medicine, N.Y., N.Y. 10029, *Univ. of CT, Farmington, 06032

The intracellular Ca Release channel (ryanodine receptor, RyR) is activated in processes as diverse as fertilization and muscle contraction. Recombinant RyR, expressed in insect cells (Sf9), was purified and incorporated into Fluo-3 loaded liposomes. Fluorescence measurements revealed Ca-induced Ca influx into liposomes that was inhibited by ruthenium red (RR). Single channel properties of the cloned expressed RyR, in liposomes fused into planar bilayers, revealed a full conductance of 515±57 pS (CsCl gradient 250/50 mM), comparable to the native channel. Full conductance was observed in 4/32 experiments, in 28 experiments expressed channels opened to subconductance levels. In all cases expressed channels responded to compounds known to modulate RyR function. The channel was activated by caffeine, ATP and Ca, and was inhibited by RR and Mg. Ryanodine modified the channel to open to the characteristic subconductance state with slowed kinetics. We conclude that expression of the RyR in non-mammalian cells produces functional Ca release channels that respond to modulators of the native RyR.

W-AM-A2

EXPRESSION AND RECONSTITUTION OF THE CLONED AND NATIVE RABBIT SKELETAL MUSCLE CALCIUM RELEASE CHANNELS (RYANODINE RECEPTOR) IN XENOPUS OOCYTES
((E. Kobrinsky, A-M. B. Brillantes, K. Ondrias, and A.R. Marks)) Mount Sinai School of Medicine, N.Y., N.Y. 10029

The function of the cloned expressed Ca release channel/ryanodine receptor (RyR1) was characterized in *Xenopus* oocytes injected with *in vitro* transcribed RNA (5 to 50 ng). Oocyte responses to channel modulators were determined by recording the endogenous Ca-activated Cl current at a holding potential of -60 mV. In injected oocytes, but not in control (uninjected), caffeine (5 to 50 mM) evoked dose-dependent intracellular Ca release (Ca-activated Cl current = 132 ± 36 nA, n = 20). Ryanodine (100 nM) elicited intracellular Ca-release (Ca-activated Cl current = 233 ± 17 nA, n = 3) only in injected oocytes and only after preactivation with caffeine (10 to 50 mM). Caffeine and ryanodine induced Ca release from the same intracellular pool. Injection of rabbit skeletal muscle heavy sarcoplasmic reticulum (SR) fraction (500ng/oocyte) resulted in functional reconstitution of the native RyR1 with properties similar to those of the cloned expressed channel. We conclude that the skeletal muscle RyR1 cDNA encodes the functional SR Ca-release channel, and that direct injection of native RyR1 protein into oocytes provides a useful model for comparing properties of the cloned versus native channels.

W-AM-A3

[^{3}H]RYANODINE BINDING STUDIES OF CALSEQUESTRIN-DEPLETED HEAVY SARCOPLASMIC RETICULUM (HSR) SUPPORT A REGULATORY ROLE OF CALSEQUESTRIN ON THE RYANODINE RECEPTOR/Ca^{2+} RELEASE CHANNEL. ((D.M. Vaughan, J. Ervasti and R. Coronado)) Dept. of Physiology, Univ. of Wisconsin Medical School, Madison, WI 53706.

We studied the effect of calsequestrin on the ryanodine receptor/Ca^{2+} release channel by comparing [^{3}H]ryanodine binding to calsequestrin-depleted and normal HSR from rabbit skeletal muscle. Calsequestrin-depleted HSR (HSR-CS) was formed by incubation in a solution containing Tris/EGTA, followed by centrifugation. SDS-PAGE of the pellet and supernatant revealed that about 80% of the calsequestrin was removed from the pellet. A few minor components in addition to calsequestrin were present in the supernatant. The pCa of all solutions was adjusted to 6, and [^{3}H]ryanodine binding to solubilized vesicles in the absence or presence of the supernatant was measured. In four experiments, each using triplicate determinations, HSR-CS bound approximately two times more [^{3}H]ryanodine than HSR. Addition of the supernatant to HSR-CS resulted in a return of the binding toward control levels, while a similar addition to HSR caused no significant change in binding. Since [^{3}H]ryanodine binding is used as an indicator of the open probability of the ryanodine receptor/Ca^{2+} release channel, these studies provide additional evidence for a regulatory role of calsequestrin on the Ca^{2+} release channel of sarcoplasmic reticulum. (Supported by NIH, MDA and AHA.)

W-AM-A4

RADIOIMMUNOASSAY FOR THE CALCIUM RELEASE CHANNEL AGONIST RYANODINE. ((S.D. Kahl[1], P.S. McPherson[1], T. Lewis[2], P. Bentley[2], M.J. Mullinnix[1], J.D. Windass[2] and K.P. Campbell[1])) [1]Howard Hughes Medical Institute, Dept. of Physiology and Biophysics, University of Iowa College of Medicine, Iowa City, Iowa 52242. [2]Zeneca Agrochemicals, Jealott's Hill Research Station, Berks, England RG12 6EY. (Spon. by R. Fellows)

The ryanodine receptor/Ca^{2+} release channel is involved in intracellular calcium homeostasis in both muscle and nonmuscle cells. Ryanodine, a neutral plant alkaloid, is capable of specifically interacting with this Ca^{2+} release channel. A novel photo-activatable derivative of ryanodine, 9-hydroxy-21-(4-azidobenzoyloxy)-9-epiryanodine, has been synthesized and conjugated to keyhole limpet hemocyanin (KLH) for the production of antibodies with high affinity and specificity to ryanodine. The anti-ryanodine antibodies reacted specifically on immunoblots with the azido-ryanodine compound covalently conjugated to bovine serum albumin (BSA). A radioimmunoassay specific for ryanodine and ryanodine derivatives was developed using the anti-ryanodine antibodies. Using the radioimmunoassay, a dissociation constant for ryanodine of 1 nM was determined. The introduction of bulky groups at C_{21} of ryanodine was detrimental to binding indicating that a substitution of this nature may sterically hinder binding to the anti-ryanodine antibodies. In contrast, bulky substituents at C_{10} of ryanodine can be tolerated with little effect on binding. Half-maximal inhibition constants (IC_{50}) for various ryanodine derivatives were found to range between 3.2 nM and 200 nM. These IC_{50} values correlated very well with the IC_{50} values obtained for the compounds binding to the skeletal muscle membrane receptor. In summary, a photoactivated ryanodine derivative has been produced and used to generate anti-ryanodine antibodies which have high affinity and specificity for ryanodine and which exhibit binding properties similar to the skeletal muscle membrane receptor. These antibodies should be useful for the characterization of the ryanodine binding site on the sarcoplasmic reticulum Ca^{2+} release channel.

W-AM-A5

PHOTOAFFINITY LABELING OF THE RYANODINE RECEPTOR/CA^{2+} RELEASE CHANNEL WITH AN AZIDO DERIVATIVE OF RYANODINE. ((D.R. Witcher[1], P.S. McPherson[1], S.D. Kahl[1], T. Lewis[2], P. Bentley[2], M.J. Mullinnix[1], J.D. Windass[2] and K.P. Campbell[1])) [1]Howard Hughes Medical Institute, Dept. of Physiology and Biophysics, University of Iowa College of Medicine, Iowa City, Iowa 52242. [2]Zeneca Agrochemicals, Jealott's Hill Research Station, Berks, England RG12 6EY.

Ryanodine receptors play an important role in regulating the intracellular calcium concentrations in both muscle and non-muscle cells. Ryanodine, a neutral plant alkaloid, specifically binds to and modulates the ryanodine receptor/Ca^{2+} release channel. We have characterized the interaction of a tritium-labeled, photoactivatable azido-benzamide derivative of ryanodine (ABRy) to skeletal, cardiac, and brain membranes. Scatchard analysis demonstrates that [^{3}H]ABRy binds to a single class of sites in skeletal muscle triads with a K_d and B_{max} of 5.5 nM and 12.7 pmol/mg, respectively. Furthermore, binding assays with [^{3}H]ryanodine to skeletal, cardiac, and brain membranes in the presence of increasing concentrations of unlabeled ABRy illustrates that this azido derivative of ryanodine is able to specifically displace [^{3}H]ryanodine from its binding site(s). Analysis of the effects of Ca^{2+}, ATP, and KCl on [^{3}H]ABRy binding in triad membranes shows a similar modulation of binding as seen in these membranes with [^{3}H]ryanodine. Both ruthenium red and Mg^{2+} prevented photolabeling of the skeletal muscle ryanodine receptor with [^{3}H]ABRy. These results demonstrate that [^{3}H]ABRy binds to the same site in triads as [^{3}H]ryanodine, and that this binding is allosterically regulated by KCl, ATP, Ca^{2+}, ruthenium red, and Mg^{2+}, compounds known to directly affect Ca^{2+} release from the ryanodine receptor. Photoaffinity labeling of triads with [^{3}H]ABRy resulted in specific and covalent incorporation of [^{3}H]ABRy into a 560,000 kDa protein. This protein was identified with specific polyclonal antibodies to skeletal muscle ryanodine receptor. [^{3}H]ABRy should be a useful tool for identifying the binding site for ryanodine and for determining the presence of other ryanodine receptors.

W-AM-A6

FUNCTIONAL DOMAINS OF THE SKELETAL MUSCLE RYANODINE RECEPTOR: IDENTIFICATION OF CALMODULIN BINDING SEQUENCES. ((P. Menegazzi, F. Larini, S.Treves, G.F. Prestipino[1], and F.Zorzato))Inst. Gen. Pathol., Univ. of Ferrara, Ferrara, Italy, [1]C.N.R., Inst. Cybernetics and Biophys. (Spon. by P. Volpe)

In this study we have identified calmodulin binding regions of the skeletal muscle ryanodine receptor Ca^{2+} release channel. We produced 30 RyR fusion proteins in the pATH expression vector. Calmodulin ligand overlay on western blots of these fusion proteins allowed us to define two calmodulin binding regions: (i) the first one encompassed a calmodulin-binding consensus sequence and is located in the large hydrophilic portion of the molecule. Binding of calmodulin was optimal at 100 nM calmodulin; (ii) the second region is located within the last 1000 COOH-terminal residues. Binding of calmodulin to the latter region was Ca^{2+} dependent and occured at concentrations of 5-100 nM. These results imply that in vivo calmodulin may interact with the ryanodine receptor, thereby modulating its activity.

W-AM-A7

LOCALIZATION OF THE RYANODINE BINDING SITE ON THE SKELETAL MUSCLE CA^{2+} RELEASE CHANNEL. ((C. Callaway, K. Slavik, J-P. Wang, D. Needleman, T. Jayaramon[1], A. Marks[1] and S.L. Hamilton)) Dept. of Molecular Physiology & Biophysics, Baylor College of Medicine, Houston, TX; [1]Dept. of Molecular Biology, Mount Sinai Medical Center, New York, NY

Upon solubilization of trypsin digested sarcoplasmic reticulum membranes, [^{3}H]-ryanodine remains bound and sediments as an ~10S complex (Meissner *et al., J. Biol. Chem.* 264:1715-1722, 1989). We have isolated and purified this 10S species. The complex retains both high and low affinity ryanodine binding sites as evidenced by the ability of excess unlabelled ryanodine to slow the dissociation of the [^{3}H]-ryanodine bound to the high affinity site on the 10S complex. Examination of the polypeptide composition of this complex reveals 4 polypeptides with apparent molecular weights of 76K, 64K, 46K and 27K. The 76K, 64K, and 27K can be labeled in Western blots with an antibody to the last 9 amino acids on the carboxy terminus. The first 10 amino acids of the 76K polypeptide are KLGVDGEEEE, indicating that the proteolytic clip occurred after Arg 4475. Examination of the time course of proteolysis of the Ca^{2+} release channel indicates that the formation of the 76K polypeptide is very rapid, occurring within 1' at 37°C with a protein to trypsin ratio of 1:1000. Subsequent to this, a cleavage converts a small amount of the 76K to the 64K and the remainder to the 27K and 46K polypeptides. Further proteolysis leads to the digestion of the carboxy terminal portion of the 27K (recognized by the antibody) to a fragment of less than 5K. Our data suggest that both the high and low affinity ryanodine binding sites are in the region of the protein between ARG 4475 and the carboxy terminus. This work is supported by grants from the National Institutes of Health and the Muscular Dystrophy Association of America.

W-AM-A8

FK-506 INFLUENCES ADAPTIVE BEHAVIOR OF THE SR RYANODINE RECEPTOR. ((S.Györke, C.Dettbarn and P.Palade)) Dept. Physiology & Biophysics, University of Texas Medical Branch, Galveston, TX 77555.

Intracellular Ca^{2+} release channels, including the inositol trisphosphate receptor (IP_3R) and ryanodine receptor (RyR) exhibit a unique adaptive behavior, characterized by the ability of the channels/receptors to respond to incremental increases in agonist concentrations by transient bursts of activity (Ferris et al., Nature 356, 350, 1992; Györke & Fill, Science 260, 807, 1993). The mechanism underlying this phenomenon is not known. One hypothesis suggested to explain incremental activation of IP_3Rs involves a hypothetical regulatory protein ("memory molecule") which is activated by the open state of the channel and promotes formation of the closed or "inactivated" state of the channel (Swillens, Mol. Pharmacol., 41, 110, 1992). Recently it has been demonstrated that a 12 kDa FK-binding protein (FKBP) is closely associated with the RyR (Jayaraman et al., J. Biol. Chem., 267, 9474, 1992). FKBP is a cis-trans isomerase; thus it could mediate adaptive behavior by inducing slow conformation changes in the RyR. To test this hypothesis, we examined the effect of the isomerase inhibitor FK-506 on Ca^{2+} release from isolated sarcoplasmic reticulum (SR) microsomes, using a conventional spectrophotometric assay. At 10-100 μM concentrations the drug potentiated caffeine-induced release in both cardiac and skeletal SR by increasing the amplitude and dramatically slowing down the descending phase of release. The drug also reduced the ability of Ca^{2+} stores to produce repeated releases in response to incremental additions of the same amounts of caffeine. At the same time it had no significant effect on Ca^{2+} uptake measured in the presence of oxalate and ruthenium red. Thus, FK-506 interferes with the ability of the Ca^{2+} release to evince apparent inactivation/adaptation and incremental activation. These results support the hypothesis that adaptive behavior is mediated by FKBP, although further experiments will be required to determine whether the effects seen are mediated by the FKBP or represent direct effects of FK-506 on the RyR.

W-AM-A9

ACTIVATION AND INACTIVATION OF THE CALCIUM RELEASE CHANNEL (CRC) OF SARCOPLASMIC RETICULUM (SR) FROM SKELETAL MUSCLE AND HEART. ((Jürgen Hain[+], Sati Nath[*], Alois Sonnleitner[+], Sidney Fleischer[*] and Hansgeorg Schindler[+])) [+]Institute of Biophysics, University of Linz, A-4040 Linz, Austria; and [*]Department Molecular Biology, Vanderbilt University, Nashville, TN 37235 USA.

The activity of the CRC was studied after incorporation of SR vesicles into planar bilayers. The CRCs from both skeletal muscle and heart were modulated by a variety of conditions in similar ways. 1) Cyclic application of protein kinase A (PKA) or Ca^{2+}/calmodulin dependent protein kinase II (CaIPK) and potato acid phosphatase (PPT) or protein phosphatase I (PPT I) revealed that only the dephosphorylated state of the channel is blocked by mM free Mg^{2+}. That is, the Mg^{2+} block can be removed by phosphorylation with added PKA or CaIPk and the channel again inactivated by treatment with protein phosphatases. 2) At mM free Mg^{2+} and ATP, which approximates conditions in the myoplasm, the CRC activity induced by PKA application was not dependent on [Ca^{2+}]. 3) Activation of endogenous CaIPK (end CaIPK) led to channel closure which could be reversed by further phosphorylation by added CaIPK, or by dephosphorylation using protein phosphatases. 4) Calmodulin by itself, without activation of end CaIPK, blocks PKA phosphorylated channels, but not CaIPK phosphorylated channels. Our findings indicate, for both skeletal muscle and heart CRCs, multiple sites of phosphorylation with different functional consequences which may be relevant to excitation-contraction coupling. Supported by Austrian Research Fonds, grants S-45/03,07 (JH and HS) and by NIH HL 32711 (SF).

W-AM-A10

RAPID COOLING AND ALKALINE-INDUCED Ca^{2+} RELEASE FROM CARDIAC SR OCCURS IN THE PRESENCE OF RYANODINE BLOCKADE ((J.J.Feher)) Medical College of Virginia, Richmond VA 23298 (Spon. by G. Ford)

Rapid-cooling contractures in cardiac muscle preparations are thought to be caused by the release of Ca^{2+} from the SR, but the mechanism of the release is unknown. We studied rapid-cooling and pH-jump Ca^{2+} release using isolated dog cardiac SR and millipore filtration. After active loading to steady-state, rapid cooling resulted in the net release of Ca^{2+} which is sufficient to account for rapid-cooling contracture. The release of Ca^{2+} appeared to be a relaxation between steady-state levels of Ca^{2+} uptake. The rapid-cooling release was also observed when ryanodine or ruthenium red blocked the ryanodine-sensitive Ca^{2+} efflux pathway. In the presence of ryanodine, the extent and initial rate of Ca^{2+} efflux was increased due to the increased steady-state uptake, but the first-order rate constant for rapid-cooling Ca^{2+} release was unchanged. This suggests that rapid-cooling Ca^{2+} release does not occur through the ryanodine-sensitive pathway. The rapid-cooling release is accompanied by an alkalinization due to the temperature dependence of the K_a of the imidazole buffer. The imidazole buffer was chosen specifically to match the temperature-dependence of most intracellular buffers, and so to mimic the pH change of intact preparations upon cooling. The alkalinization was not the major cause of rapid-cooling Ca^{2+} release, as comparable Ca^{2+} release was also observed with rapid cooling with no alkalinization (produced by simultaneous cooling and addition of HCl). However, in separate experiments, alkalinization without rapid cooling produced a rapid net Ca^{2+} release which was also observed in the presence of ryanodine. The pH-jump Ca^{2+} release was graded, being 14 nmol/g with ΔpH = 0.2 and 30 nmol/mg with ΔpH = .48. These net releases were complete within 6 s. The pathway for the rapid-cooling and pH-jump Ca^{2+} efflux remains to be identified.

W-AM-B1

TOPOLOGICAL MAPPING OF PHOSPHOLEMMAN WITH USE OF SITE-SPECIFIC ANTIBODIES. ((S. E. Cala and L.R. Jones)) Krannert Institute of Cardiology and the Department of Medicine, Indiana University School of Medicine, Indianapolis, IN 46202

Phospholemman (PLM) is a 72-amino acid phosphoprotein that is believed to function as a Cl^- channel in heart and several other cell types. Phosphorylation sites for cyclic AMP-dependent protein kinase and protein kinase C are contained in the cytosolic portion of the molecule (residues 38-72). Hydropathy analysis predicts a single hydrophobic domain (residues 18-37) and an extracellular amino-terminal portion (residues 1-17). We have investigated the topology of phospholemman in purified cardiac sarcolemmal (SL) vesicles using antibodies directed against either an amino- or carboxyl-terminal peptide (15-mers). Immunoblot analyses of phospholemman following treatments of SL with any of several proteases revealed a complete loss of the carboxyl terminus (only in the presence of detergent) but no apparent loss of the amino terminus. Interestingly, with cleavage of the carboxyl-terminal end of the molecule, the anomalous mobility of phospholemman by SDS-PAGE (M_r [intact protein] = 15,000) was largely maintained. Very similar results were obtained using recombinant phospholemman made with the baculovirus expression system and purified by immunoaffinity chromatography in detergent. These data suggest that the amino-terminal half of phospholemman exhibits a protected configuration in membranes and detergent micelles. Studies are in progress to determine if this region of the molecule accounts for the Cl^- channel activity.

W-AM-B2

MEMBRANE TOPOLOGY OF FUNCTIONAL AQUAPORIN CHIP MOLECULES. ((G.M. Preston, J.S. Jung, W.B. Guggino, and P. Agre)) Johns Hopkins Univ. School of Medicine, Baltimore, MD 21205.

CHIP is the archetypal member of the Aquaporins, a widely expressed family of membrane water channels. The NH_2- and COOH-terminal halves of CHIP are sequence-related, and hydropathy analysis predicted six membrane spans with five connecting loops (A-E). Here we report the direct demonstration of the membrane topology of CHIP expressed in *Xenopus* oocytes using biologically active recombinant channels. CHIP is glycosylated at Asn-42, indicating loop-A is exofacial. An epitope from the coronavirus E1 glycoprotein was inserted into CHIP and localized to the outer or inner leaflet of the membrane by α-chymotrypsin digestion of intact oocytes or inside-out membrane vesicles. The E1 epitope at Thr-120 was protease-sensitive in intact oocytes, indicating loop-C is exofacial. The E1 epitope at Lys-6, Arg-162, or Lys-267 was protease-sensitive in inside-out membrane vesicles, confirming the cytoplasmic location of the NH_2- and COOH-termini and loop-D. Insertions into loops-B and -E did not produce active water channels, but their cleavage patterns were consistent with inner (B) and outer (E) leaflet locations. These studies indicate that the functional CHIP molecule is a unique structure with two internal repeats oriented 180° to each other in a membrane.

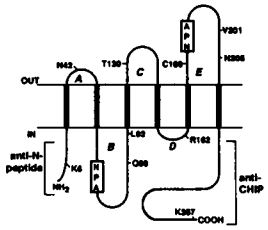

W-AM-B3

BIOLOGICALLY ACTIVE TWO-DIMENSIONAL CRYSTALS OF AQUAPORIN CHIP. ((T. Walz, B.L. Smith, M.L. Zeidel, P. Agre, and A. Engel)) M.E. Müller-Inst., Biozentrum, Basel, Switzerland CH-4056; Johns Hopkins Univ. School of Med., Baltimore, MD 21205; Univ. Pittsburgh School of Med., Pittsburgh, PA 15213. (Spon. by S. Ambudkar)

The 28 kDa red cell channel-forming integral protein CHIP is the archetypal member of the Aquaporins, a family of water-selective channels widely distributed among plants and mammals. The structure of CHIP was not previously well characterized; here we define it to a resolution of 1.6 nm in biologically active 2-D protein-lipid crystals. Visualized by single particle averaging, negatively stained purified CHIP oligomers in octyl-ß,D-glucopyranoside (OG) exhibited a distinct 4-fold symmetry and a side length of 10 nm. A mass of 202±3 kDa was determined by scanning transmission electron microscopy, consistent with a tetramer comprised of three 28 kDa subunits, one 50 kDa glycosylated subunit, and 225 OG molecules. When reconstituted at lipid:protein=1, CHIP formed 3 μm diameter vesicles with highly ordered 2-D square arrays with full biological activity, $5x10^{-14}$ ml/sec/CHIP. The crystals have a mass/area=4.1±0.27 kDa/nm^2, unit cell of dimensions a=b=9.6 nm, and P422$_1$ symmetry. The calculated 378 kDa unit cell mass enclosed two CHIP tetramers and adjacent phospholipids. The 3-D map calculated from a tilt series of uranyl formate stained square arrays revealed central depressions extending from both sides of the membrane deep into the transbilayer domain of the CHIP tetramer, leaving only a thin barrier to be crossed by narrow segments of the aqueous pathways. Although CHIP monomers may contain individual water pores, the stability and function of the protein must require the highly uniform tetrameric membrane organization.

W-AM-B4

MOLECULAR DOMAINS OF THE WATER-PATHWAY THROUGH AQUAPORIN CHIP: THE HOURGLASS WATER CHANNEL MODEL. ((J.S. Jung, G.M. Preston, B.L. Smith, W.B. Guggino, and P. Agre)) Johns Hopkins Univ. School of Medicine, Baltimore, MD 21205. (Spon. by P. Pedersen)

The internal structures responsible for the water pathway in the Aquaporin CHIP molecule remain undefined. Previous comparisons revealed that the NH_2- and COOH-terminal halves of CHIP are sequence-related and oriented at 180° to each other when within the membrane. Moreover, each half of CHIP contains the motif NPA (residues 76-78 in endofacial loop B; residues 192-194 in exofacial loop E). The sequences of loops B and E are very hydrophobic, and scanning mutagenesis studies revealed these domains to be highly intolerant of substitions when measured by the *Xenopus* oocyte osmotic swelling assay. Conservative substitutions of greater mass at corresponding points in loops B and E resulted in equivalent reductions in P_f. C189 (loop E) is known to be the residue responsible for reversible inhibition by mercury, since C189S was fully active and resistant to inhibition. A73 (loop B) corresponds to C189, and the mutant A73C,C189S exhibited wild-type P_f which was fully inhibitable by mercury. As expected, coexpression of non-functional mutants in loop B and loop E failed to complement each other, but certain mutants fully complemented other nonfunctional CHIP recombinants resulting from mutations in other domains. These results indicate that the NPA motifs and the adjacent residues 73 and 189 are located near a narrowing of the water-pathway, and modifications at either site will occlude the pore. The simplest model explaining these studies is an hourglass with an endofacial chamber (loop B) and and exofacial chamber (loop E) with NPA domains which overlap between the leaflets of the lipid bilayer.

W-AM-B5

IMAGE ANALYSIS OF RECONSTITUTED CYTOCHROME c OXIDASE VISUALISED BY Pt/C AND BY W/Ta SHADOWING. ((M.Tihova, B.Tattrie and P.Nicholls)) Department of Biological Sciences, Brock University, St.Catharines, Ont. L2S 3A1, Canada

Incorporation of beef heart cytochrome oxidase into phospholipid vesicles by cholate dialysis creates catalytically functional proteoliposomes. The individual inlaid complexes have been observed by freeze-fracture electron microscopy. Pt/C shadowing has directly confirmed the asymmetrical protrusion of the enzyme particles. By using image analysis the areas and heights for the dimer, monomer and oligomer forms at the cytochrome c binding side and at the matrix-facing side have been measured. The size distribution profiles of the enzyme particles are affected by changing the phospholipid composition and the L/P ratio (Biochem.J., 1993, **292**, 933-946).
W/Ta shadowing has revealed some additional features of the embedded enzyme complexes. The estimated areas of the dimers and of the monomers depend on the delineation of a poorly defined protein-lipid boundary. At the center of each projection is a small extra protrusion. The protein complexes are surrounded by an area of the liposome surface with a modified texture. The number of the modified phospholipid molecules in each surrounding domain has been calculated. The presence of protein may immobilise the surrounding phospholipid molecules and thus provide a nearly constant microenvironment for enzyme activity.
Supported by NSERC Canada grant #A-0412 to Peter Nicholls.

W-AM-B6

THE STRUCTURE AND THERMAL UNFOLDING OF BEEF-HEART MITOCHONDRIAL CYTOCHROME OXIDASE AS STUDIED BY FOURIER-TRANSFORM INFRARED SPECTROSCOPY. ((J.L.R. Arrondo, J. Castresana, J.M. Valpuesta and F.M. Goñi)) Departamento de Bioquímica, Universidad del País Vasco, Aptdo. 644, E-48080 Bilbao, Spain.

Fourier-transform infrared spectroscopy has been applied to the study of lipid vesicle-supported two-dimensional crystals and non-crystalline preparations of beef-heart cytochrome oxidase. At room temperature, no conformational differences are seen between the amorphous and crystalline proteins, whose conformation is shown to consist of ca. 40% α-helix, 20% extended structures (including ß-sheet), 17% ß-turns, 17% loops, and 5% non-structured. Upon heating the protein from 20 to 80ºC, a major thermal event occurs, centered at 55-60ºC, leading to a compact denatured state, devoid of enzyme activity. Thermal denaturation is accompanied by a decrease in unordered structure and an increase in ß-turns, without major changes in the proportion of α-helix. Temperature-induced changes are not the same in amorphous and crystalline structures, the latter being in general more stable towards the thermal challenge. The above data extend and confirm previous structural studies on cytochrome oxidase using cryoelectron microscopy.

W-AM-B7

STRUCTURAL AND THERMAL CHARACTERIZATION OF MEMBRANE BOUND AND SURFACE ADSORBED PROTEIN. ((J. Wang[a], C.J.A. Wallace[b], I. Clark-Lewis[c] and M. Caffrey[a])) [a]Chemistry, The Ohio State University, Columbus, OH 43210, [b]Biochemistry, Dalhousie University, Halifax, Nova Scotia, Canada B3H 4H7 and [c]Biomedical Research Center, University of British Columbia, Vancouver, B.C., Canada V6T 1Z3.

The x-ray standing wave (XSW) method has been used to study the topology of the protein, cytochrome c, bound to a negatively charged model lipid membrane and adsorbed at a metal surface. At the metal surface, cytochrome c forms an hexagonally close-packed monolayer. A similar packing arrangement is observed at the surface of a self-assembled lipid monolayer on silver. In the case of a Langmuir-Blodgett (LB) film, protein multilayers are formed. The data suggest that cytochrome c maintains its native globular structure upon surface binding and subsequent storage for an extended period. Further, the data are consistent with a protein docking mechanism wherein the heme plane is oriented perpendicular to and with its exposed edge facing the surface. The XSW measurement has also been used to show that the surface bound cytochrome c monolayer on a silver mirror surface undergoes a thermal melting transition starting *ca.* 55 °C. Unlike the unfolding transition of cytochrome c in aqueous buffer solution, this melting transition is not reversible upon cooling to room temperature. This study demonstrates the utility of the XSW method as a new and powerful structural tool for investigating membrane- and surface-protein interactions.

W-AM-B8

SELF-ASSEMBLY OF MULTILAYER LIPID STRUCTURES STABILIZED BY PROCOLIPASE ((H.L. Brockman and W.E. Momsen)) The Hormel Institute, University of Minnesota, 801 N.E. 16 th Avenue, Austin, MN 55912

Procolipase (ProCol) is a surface-active, 10,000 Da protein which anchors pancreatic lipase to bile-salt covered, lipid-water interfaces. To better understand lipid-ProCol mixing in interfaces we measured ProCol-induced surface pressure (π) changes and ProCol adsorption (Γ) to monolayers of 1-stearoyl-2-oleoylphosphatidylcholine (SOPC) and either a model lipase substrate, 1,3-dioleoylglycerol (DO), or product, 13,16-*cis,cis*-docosadienoic acid (DA). Aqueous phase ProCol, 240 nM, was saturating. At all initial π < 24 mN/m with SOPC alone, final π was ~24 mN/m and Γ was proportional to the free space created by ProCol compression of SOPC from the initial to the final π. However, this compressibility model failed to explain π and Γ changes obtained with DO- or DA-containing films. With increasing DO or DA mole fraction, final π values were in excess of the collapse π values of the monolayers in the absence of ProCol, indicating non-ideal lipid-protein interactions, and Γ's were larger than predicted. Analysis of the Γ data as a function of lipid composition using an alternative model indicated that SOPC and ProCol occupied constant areas of 70 and 708 $Å^2$, consistent with their molecular cross-sections. However, DO and DA occupied areas of 18 and 14 $Å^2$, 1/3 and 1/2 the expected values. These results were obtained whether the data were analyzed stepwise, with respect to lipid composition, or in aggregate and indicate ProCol stabilization of multilayer structures. The energetically favorable interaction of ProCol with DO and DA to form lipid multilayers suggests that ProCol may play the previously unrecognized role of recruiting substrate, but not SOPC, to the interfacial lipase-ProCol complex. (Supported by NIH HL-49180)

W-AM-B9

DYNAMICAL PROPERTIES OF LIPIDS FROM *SARCINA VENTRICULI* GROWN UNDER ENVIRONMENTAL STRESS. ((Luc R. Berubé and Rawle I. Hollingsworth)) Biochemistry dept. and Center for Microbial Ecology, MSU, East Lansing, MI 48824.

Sarcina ventriculi, a strictly anaerobic bacterium, was grown at pH 3.0 and pH 7.0. At pH 3.0 the bacterium produces ethanol and synthesizes unusual long chain fatty acids that are able to span the bilayer. We tested the hypothesis that the presence of those long chain fatty acids is necessary to maintain the dynamical properties of the membrane under stress. Lipids were extracted and resuspended in aqueous buffer and subjected to NMR T_1 relaxation time (T_1) measurements and dipolar echo decay spectrometry (DECODE). We found that T_1 values for methylene protons of the lipid system containing the long chain fatty acids and maintained at pH 7.0 were lower at all temperatures tested when compared to the lipid system from cells grown at pH 7.0. Arrhenius plots revealed that the energy of activation (Ea) for T_1 was also lower. When the lipids containing the long chain fatty acids were suspended in pH 3.0 buffer, the Ea remained the same as the one observed at pH 7.0. However, addition of 0.6 M methanol resulted in the Ea being similar to the Ea observed for the lipids from cells grown at pH 7.0 and maintained at pH 7.0. DECODE spectroscopy suggested that these two lipid systems (from cells grown at pH 3 and maintained at pH 3 with methanol and from cells grown at pH 7 and maintained at pH 7), eventhough they have similar Ea, have different molecular organization. It is concluded that Ea for T_1 relaxation may reflect important dynamical properties of membranes that need to be preserved for optimal membrane activity. (Supported by DOE grant# DE-FG0289ER14029 to R.I.H and by a fellowship from the Center for Microbial Ecology, a NSF Science and Technology Center to L.R.B)

W-AM-B10

INTERACTION OF MK-801 WITH BIOLOGICAL AND MODEL MEMBRANES ((Jill Moring, Lesley Niego, and Leo Herbette)), University of Connecticut Health Center, Farmington, CT 06030

MK-801 (dizocilpine, (5R,10S)-(+)-5-methyl-10,11-dihydro-5H-dibenzo[a,d]cyclohepten-5,10-imine) is a noncompetitive antagonist of the NMDA receptor. It is thought to bind to the activated (open) state of the cation channel associated with the NMDA receptor, the specific binding site being located in the hydrophobic region of the bilayer. Because of its useful characteristics, which include apparent protective effects against excitotoxicity and ability to mitigate seizures in animals after withdrawal from chronic ethanol, MK-801 or similar agents might have therapeutic applications. Understanding the membrane interactions of MK-801 might be important in the design of drugs with similar properties.

We have investigated the interaction of MK-801 with native synaptoneurosomal membranes (SNM) from rat cerebral cortex, and with multilamellar and unilamellar cholesterol/dioleoylphosphatidylcholine (DOPC) liposomes. MK-801's association with and dissociation from model and native membranes were rapid. Partition coefficients ($K_{P[mem]}$) were relatively low: $K_{P[mem]}$ (± S.D.) = 428 (± 118) in SNM, and 661 (± 264) in cholesterol/DOPC (multilamellar liposomes, mole ratio 0.6). Decreasing the cholesterol content increased $K_{P[mem]}$.

Small angle x-ray diffraction experiments conducted at a high membrane hydration state show that MK-801 perturbs the headgroup region of cholesterol/DOPC membranes (mole ratio = 0.6) at ~16 Å from the bilayer center. These characteristics are consistent with a relatively fast onset and short duration of action and with approach of the drug to its binding site through the hydrated region of the membrane and the aqueous region. Supported by NIAAA #5K21-AA0126.

PHOTOSYNTHETIC PROTEINS

W-AM-C1

KINETIC RESOLUTION OF SPECTRALLY DISTINCT b_h AND b_l HEMES IN THE b_6f COMPLEX OF STROMAL VESICLES FROM SPINACH CHLOROPLASTS. ((J.G. Fernandez-Velasco, E.A. Berry* and R. Malkin)) Dept. Plant Biology, 461 Koshland Hall and * Lawrence Berkeley Lab.,Building 1. Univ. of California. Berkeley, CA 94720.

The thermodynamic and spectral heterogeneity of the b_6f complex b hemes have been previously shown in chloroplasts (1) and stromal membranes (2) by dark equilibrium redox titrations. Here we show the spectrally distinguishable flash induced redox changes of the b_h and b_l hemes in stromal membranes. The time resolved redox differential spectra (1-2500 ms) indicate, for all E_hs, that the peak of cyt b_h and b_l is at 563 and 565.5 nm, respectively. In spite of this small difference, when both hemes are initially oxidized or reduced in the dark and then photoreduced or photooxidized, respectively, both peaks or shoulders are seen. In these vesicles, with no active P680 and ca. 10 P700/b_6f, (gramicidin; pH 7; 25 C) an inter-heme electron transfer is demonstrated from the differential kinetics at various redox potentials, as follows: 1) At E_h 30 to 0 mV, where both hemes are initially oxidized, an almost simultaneous (not resolved) photoreduction of them is seen; the reaction is complete in ca. 10 ms. In variance, b_l suffers a faster net reoxidation ($t_{1/2}$ 30ms) than b_h ($t_{1/2}$ >90ms, not resolved). 2) At -230 mV, where both hemes are reduced in the dark , and after an apparent lag of ca. 20 ms, a net photooxidation of b_l that is faster than that of b_h occurs ($t_{1/2}$ 30 ms vs > 60 ms, not resolved). Both shoulders reach the same level of bleaching after 350ms, thereafter b_h rereduces($t_{1/2}$ 3 sec) faster than b_l. 3) At ca. -100 mV, where b_h and b_l are almost fully reduced and oxidized, respectively, in the dark, only b_l shows to be photoreduced and only after it reoxidizes fully a net photooxidation of b_h develops. At this E_h stigmatellin, an inhibitor of the Q_O site, blocks cyt f rereduction and b_l photoreduction but does not impair b_h photooxidation. 4) At 140 mV (oxidized PQ_A pool) none of the spectral features assigned here to the b hemes redox changes are observed. Ref. (1) Kramer and Crofts (1990) in Baltscheffsky (ed). Cur. Res. Photosynth. 3, 283-286, Kluwer (2) Baroli, Fernandez-Velasco and Crofts (1990) Biophys. J. 59, 145 a.

W-AM-C2

ELECTRON TRANSFER FROM CYTOCHROME F TO P700 IN THE CYANOBACTERIUM *SYNECHOCYSTIS* - STUDIES IN WILD TYPE AND MUTANT STRAINS LACKING THE INTERMEDIATE ELECTRON CARRIERS PLASTOCYANIN AND CYTOCHROME C553

((Sabine U. Metzger[1], Yong Kong[1], Lili Zhang[1], Himadri B. Pakrasi[3], John Whitmarsh[1,2])) [1]University of Illinois; [2]ARS/USDA, Urbana, IL; [3]Dept. of Biology, Washington University, St. Louis, MO

We are investigating electron transfer between the cytochrome bf complex and photosystem I. Two mutants of the cyanobacterium *Synechocystis* sp. PCC. 6803 have been created[1,2] that lack either cytochrome c553 or plastocyanin. By controlling the copper concentration of the growth medium we can grow mutant cells that lack both cytochrome c553 and plastocyanin. To our surprise the cells grow photoautotrophically and sustain normal rates of oxygen evolution and dark respiration. We are using spectrophotometric measurements to track the electron transport between the cyt bf complex and PS I. By analysis of the oxidation kinetics of cytochrome f and the rereduction kinetics of the reaction center molecule of PS I we hope to determine how electrons are transferred in the absence of the known carriers.

[1,2] Lili Zhang et al. ; [1]JBC 1992 Vol. 267 No. 27 pp. 19054-19059; [2] JBC, in press

W-AM-C3

FLUORESCENCE IMAGING OF SINGLE PROTEINS

((Robert C. Dunn, Errol V. Allen and X. Sunney Xie)) Pacific Northwest Laboratory, P. O. Box 999, MS K2-14, Richland WA. 99352.

Recent advances in near-field optical microscopy offers exciting possibilities for conducting molecular spectroscopy at the nanometer dimension. The technique involves scanning a spot of light, of dimension much smaller than the optical wavelength, in close proximity to the surface of a sample. For biological applications, fluorescence measurements with near-field optics is particularly informative, providing spectroscopic information not accessible with other scanning probe techniques such as SEM, STM and AFM.

In our efforts to study photosynthetic proteins, we have recently obtained fluorescence images from single allophycocyanin trimers dispersed on a glass surface [R. C. Dunn, E. V. Allen, S. A. Joyce, G. A. Anderson, X. S. Xie, J. Ultramicroscopy, in press]. Images show emission features with 100nm FWHM which are attributable to single proteins containing only six tetrapyrrole chromophores. The spatial resolution is only limited by the size of the probe. This result demonstrates the single protein sensitivity and spatial resolving power of our near-field microscope. Furthermore, our results indicate that the emission from a single APC trimer is enough to spread the counts in both the frequency and time domains. We are currently collecting the emission spectrum of single APC trimers and implementing fluorescence polarization spectroscopy to obtain structural information. Furthermore, we are incorporating a picosecond time-correlated single photon counting ability into our microscope. Lifetime imaging not only provides intrinsic information free from many of the complications inherent in intensity imaging but will also allow us to measure dynamical events such as electron and energy transfer in photosynthetic systems. Progress along these directions will be presented.

W-AM-C4

ORIENTATION OF THE REDUCED IRON-SULFUR CENTERS F_A AND F_B FROM LOW-TEMPERATURE EPR ON SINGLE CRYSTALS OF PHOTOSYSTEM I.
((A.van der Est, P.Fromme, A.Kamlowski and D.Stehlik)) Phys.Dep, FU and MVI, TU Berlin, D 14195 Berlin. (Spon. by K.Sauer)

Previously we have demonstrated with photoreduced F_A [1] that orientation dependent EPR at 10K can be performed in single crystals of Photosystem I from Syn.sp., for which a 3D-structure at 6Å resolution is now available [2]. We have extended this study to reduced F_B, which can be generated in more favorable competition to F_A by photoreduction at elevated temperature. The angles of two g-tensor principal axes of F_B (g_z=2.067 and g_x=1.886) with respect to the crystalline c-axis (normal to the membrane plane) are directly obtained from the rotation pattern. As for F_A [1], additional but well founded assumptions permit us to deduce the orientation of each of the distorted [Fe4S4]-cubes and their magnetic axes with respect to the crystal axes. The relative orientation of F_A and F_B in the PsaC-protein is of particular interest. The structural homology between PsaC and bacterial ferredoxin of P.aerogenes [3] predicts nearly colinear axes for the F_A and F_B clusters. In contrast, a close to perpendicular relation is concluded from our EPR-data. The structural homology can be maintained by postulating a different relative location of the mixed-valence Fe-pair in the reduced F_A and F_B centers. Consequences for the electron transfer mechanism via PsaC can be addressed. Constraints can be given for the orientation of the PsaC (if homologous to bacterial ferredoxin) with respect to the PSI reaction center core.

[1] K.Brettel et al., Biochim.Biophys.Acta, 1098 (1992) 266-270
[2] N.Krauss et al., Nature, 361 (1993) 326-330
[3] H.Oh-oka et al., J.Biochem., 103 (1988) 962-968 and others.

W-AM-C5

^{1}H ENDOR AND ^{14}N ESEEM OF P700$^{+\cdot}$ IN SINGLE CRYSTALS OF PHOTOSYSTEM I FROM *SYNECHOCOCCUS ELONGATUS**

((H. Käß, P. Fromme, H.T. Witt and W. Lubitz)) Max-Volmer-Institut, Techn. Univ. Berlin, Str. d. 17. Juni 135, D-10623 Berlin, Germany

^{1}H ENDOR spectra of the primary donor cation radical P700$^{+\cdot}$ in photosystem I (PS I) preparations of *Synechococcus* have been obtained in frozen solutions and in single crystals, see figure. Large crystals (space group $P6_3$) were grown as described in [1], yielding hexagonal plates (1.4 x 0.8 mm), for X-ray structure see [2]. Due to the complexity of the single crystal ENDOR spectra only a few hyperfine couplings could be assigned so far (methyl groups). A preliminary interpretation indicates that P700$^{+\cdot}$ is a chlorophyll dimer in which the unpaired electron predominantly resides on one half ($\geq$75%). Supporting evidence for such an interpretation is obtained from ESEEM data of the nitrogens in P700$^{+\cdot}$.

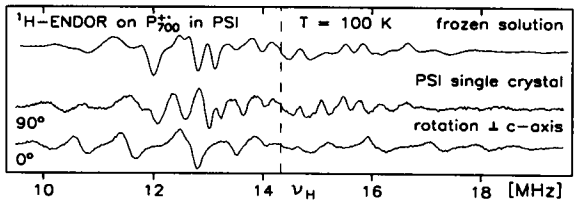

[1] Witt, H.T. et al. in Res. in Photosynth. (N. Murata, ed.), Vol. I, Kluwer, p. 521 (1992); [2] Kraus, N. et al. Nature 361, 326 (1993) *supported by DFG (Sfb 312)

W-AM-C6

THE EFFECT OF PLATINIZATION ON EXCITATION TRANSFER DYNAMICS AND P700 PHOTOOXIDATION KINETICS IN ISOLATED PHOTOSYSTEM I.

((James W. Lee*, Thomas G. Owens+, Philip D. Laible+ and Elias Greenbaum*))
*Oak Ridge National Laboratory, Oak Ridge, TN 37831
+Cornell University, Ithaca, NY 14853

Isolated Photosystem I (PSI) reaction center complexes containing about 40 chlorophylls per P700 (PSI-40) were platinized by reduction of $[PtCl_4]^{2-}$ at 20°C and neutral pH. The presence of metallic platinum on PSI complexes was detected kinetically by its effect of actinic shading and electronic shielding on P700 photooxidation and P700$^+$ reduction. The reaction centers P700 in both platinized and unplatinized PSI-40 were repeatedly photooxidized by light and reduced by ascorbate, although with somewhat slower rates in platinized PSI due to the optical shading and the electronic shielding of platinum. The effect of platinization on excitation transfer and trapping dynamics was examined by measuring picosecond fluorescence decay kinetics in PSI-40. The excitation transfer and trapping in platinized PSI-40 were essentially the same as in the control (without platinization) PSI. These results provide direct evidence that although platinization dramatically alters the photocatalytic properties of PSI, it does not alter the intrinsic excitation dynamics and electron transfer functions of PSI.

W-AM-C7

Crystallization and x-ray diffraction to 2.9Å resolution of the reaction center complex of Photosystem II from the thermophilic cyanobacterium *Mastigocladus laminosus*

((N. Adir, T. Gilon, R. Nechushtai, E. Abresch, M.Y. Okamura and G. Feher)) Physics Dept. Univ. of Calif., San Diego, La Jolla, CA 92093-0319;

The Photosystem II reaction center (RCII) performs the primary photosynthetic reactions in all oxygenic photosynthetic organisims: electron transfer from water to the secondary acceptor quinone Q_B. An RCII complex was isolated from thylakoid membranes of the thermophilic cyanobacterium *Mastigocladus laminosus* following essentially the proceedure developed for spinach RCII (1). The isolated RCII was crystallized in the presence of a detergent mixture (dodecyl maltoside, MEGA-9 and heptane triol) from which a crystal, with dimensions of 0.4x0.1x 0.05mm grew after two months. The crystal diffracted x-rays to 2.9Å resolution. The exact polypeptide content of the RCII in the crystal is under examination. Preliminary crystallographic analysis showed that the crystal belongs to the P2 monoclinic space group. The unit cell dimensions are: 160x42x160Å; $\alpha=\gamma=90^0$, $\beta=112^0$. Processing a partial data set, (collected to 6Å resolution), resulted in an R_{merge} of 0.07.

(1) N. Adir, M.Y. Okamura, D.C. Rees and G.Feher (1992), in *Research in Photosynthesis*, Vol. II (N. Murata, ed.) pp.195-198. Kluwer Academic Publishers, Dordrect. N. Adir, M.Y. Okamura and G. Feher (1992) *Biophys. J.* 61, 101a (Abstract #586) Supported by grants from USDA, NSF and NIH.

W-AM-C8

BINDING OF CYTOCHROME C_2 TO THE REACTION CENTER FROM THE ASP-L155 → LYS AND ASP-M184 → LYS MUTANTS OF *RB. SPHAEROIDES*.*

((S.H. Rongey, A.L. Juth, G. Feher and M.Y. Okamura)) Physics Dept., Univ. of Calif., San Diego, La Jolla, CA. 92093

Cytochrome c_2 (cyt), which serves as the electron donor to the photooxidized reaction center (RC) in *Rb. sphaeroides*, binds electrostatically to acidic groups on the RC surface (1). To identify residues important for the electrostatic interaction, specific residues of the RC were changed by site-directed mutagenesis. Asp-L155 and Asp-M184 were each changed to Lys [DK(L155) and DK(M184) mutants]. To determine the effect of each mutation on the binding of cyt, the fraction of RCs with cyt bound was measured as a function of the cyt concentration. The figure shows a plot of the ratio of bound RC to free RC versus cyt concentration. The dissociation constant, K_d, equals the cyt concentration when this ratio is 1. K_d increased 10 fold (to 5μM) for DK(L155) RCs and ≈400 fold (to ≈200μM) for DK(M184) RCs over the K_d in native RCs (0.5μM). The corresponding binding energies are 0.37, 0.31 and 0.22 eV for native, DK(L155) and DK(M184) RCs, respectively. The greater reduction of the binding energy for DK(M184) RCs compared to that for DK(L155) RCs shows that Asp-M184 is more important for cyt binding than Asp-L155. (1) See e.g. D.M. Tiede, *et al.* (1993) *Biochem.* 32, 4515. *Supported by NSF & NIH.

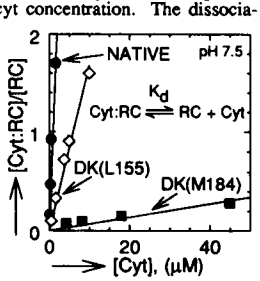

W-AM-C9

EPR STUDIES AT 35 GHZ OF Q_A^- IN SINGLE CRYSTALS OF REACTION CENTERS FROM *RB. SPHAEROIDES* R-26.* ((R. A. Isaacson, E. C. Abresch and G. Feher)) Physics Dept. Univ. of Calif., San Diego, La Jolla, CA 92093; ((F. Lendzian and W. Lubitz)) Max-Volmer-Institut, Techn. Univ. Berlin, Str. d. 17 Juni 135, D-10623, Berlin, Germany.

The g-tensor of fully deuterated Q_A^- was measured in single crystal reaction centers (RC's) of *Rb. sphaeroides* R-26 at 35 GHz in which Fe was partially replaced by Zn. The crystals were reduced with sodium dithionite and cooled to 77K. From the angular dependence of the EPR signal of Q_A^- (see Figure) the full g-tensor was obtained:

g_{xx}=2.0063(1), g_{yy}=2.0053(1), g_{zz}=2.0021(1) and direction cosines with respect to the crystal axes a,b,c :

l_{xx}= -0.13(3), 0.85(2), 0.51(2)
l_{yy}= 0.11(7), -0.50(3), 0.86(2)
l_{zz}=0.985(5), 0.169(5), -0.02(7)

for the best fit to one of the four possible sites of the unit cell. From MO calculations, the principal axis of g_{xx} is expected to lie in the quinone plane along the C-O bonds. Using the X-ray coordinates of unreduced Q_A we find an in-plane deviation of ≈10° from the C-O bond direction. [1].

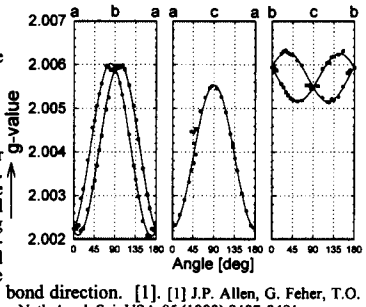

[1] J.P. Allen, G. Feher, T.O. Yeates, H. Komiya and D.C. Rees, Proc. Natl. Acad. Sci. USA *85* (1988) 8487-8491.
*Supported by NSF, NIH , DFG (Sfb 312) and NATO(CRC 910468).

W-AM-C10

CALCULATING THE pK_a OF GLU L212 IN THE PHOTOSYNTHETIC REACTION CENTER: SENSITIVITY OF THE RESULTS TO VARIATION OF PARAMETERS ((P. Beroza, D.R. Fredkin, M.Y. Okamura, and G. Feher)) Dept. of Physics, 0319, Univ. of California, San Diego, La Jolla, CA 92093.

We found that the pK_a of Glu L212, as calculated from a continuum electrostatic model, is very sensitive to variation of the model's parameters (e.g., atomic radii, protein dielectric constant, and salt concentration) and that its pK_a can vary by as much as 7 pK_a units with minor variation of these parameters.

Previous computational studies using the same continuum electrostatic model gave conflicting results: one predicted Glu L212 to be protonated in the pH range 6 to 11,[1] while another showed that Glu L212 was ionized throughout the same pH range.[2] Experimental measurements on site-directed mutant RCs suggest that Glu L212 has an anomalously high pK_a (~ 9),[3] while experimental FTIR measurements suggest that Glu L212 is ionized below pH 9.[4]

The sensitivity of the calculated pK_a to variation of parameters points out the limitations of the continuum model and helps reconcile the differences in the previously calculated pK_a's. We also find evidence for a gradual titration curve for Glu L212 and propose this as an explanation for the seemingly conflicting experimental results.

1. Cometta-Morini, et al., Int. J. Quant. Chem. Quant. Biol. Symp. 20, 89-106 (1993).
2. Gunner, M. in *the Photosynthetic Bacterial Reaction Center II*, Breton, J. and Verméglio, A., ed., Plenum Press, New York, 1992.
3. Paddock, et al., Proc. Natl. Acad. Sci. USA 86, 6602-6604 (1989).
4. Hienerwadel, et al., Biophys. J., 64, A214 (1993).
Work supported by NSF and NIH.

CALCIUM CHANNEL GATING AND REGULATION

W-AM-D1

DIRECT CALCIUM CHANNEL INHIBITION BY DISTINCT G PROTEINS.
((Andre Golard, JoAnn M. Gensert, and Steven A. Siegelbaum)) Dept. Pharmacol., Physiol., Ctr. Neuro. and Behav., Howard Hughes Medical Institute, Columbia Univ. New York, NY 10032 (Spon. by L. Zablow)

Neuronal calcium channels are inhibited by neurotransmitters in a voltage-dependent manner. The inhibition is relieved by strong depolarization, due to unbinding of a blocking particle from the channel. The rate at which channels reblock following repolarization to -80 mV is proportional to the number of active blocking particles. Although G-proteins are involved in this modulation, it is not clear whether the blocking particle is the G-protein itself or some downstream blocking particle. To address this, we studied the rate of reblock of calcium channels in NG-108 cells in the presence of modulatory transmitters. When transmitters which act through different G-proteins (Leu-Enkephalin and somatostatin) are applied simultaneously (at saturating concentrations), the rate of reblock is approximately additive while the extent of inhibition (50%) shows no additivity. The fact that inhibition is not additive implies that the two G proteins converge on a common blocking particle and/or a common population of Ca channels. However, the finding that reblock rates are additive under these conditions suggests that the G proteins act through independent pathways to modulate a common population of channels, consistent with a direct G protein-channel interaction.

W-AM-D2

L-TYPE CALCIUM CURRENT DENSITY IS REDUCED IN RAT NEONATAL VENTRICULAR MYOCYTES WITH HYPERTROPHY INDUCED BY α-ADRENERGIC STIMULATION ((John P. Gaughan and Steven R. Houser)) HYPERD and Physiology Depts. Temple University, Phila. PA 19140

Cultured rat neonatal ventricular myocytes (NVM) hypertrophy when exposed to α-agonists such as phenylephrine (P). In vivo, hypertrophy is often associated with dysfunctional electromechanical properties which can involve L-type Ca^{2+} channels. We examined if L-type Ca^{2+} channel expression is altered in NVM with hypertrophy induced by P. Low density cultures of NVM were treated with P (20 mM) or its vehicle (control) for 48 hrs. Control and hypertrophy myocytes were studied using whole cell voltage clamp. L-type Ca^{2+} currents were measured in a Na^+ and K^+ free solution containing 5 mM Ba^{2+} as the charge carrier. A holding potential of -50 mV was employed to inactivate Na^+ and T-type Ca^{2+} channels and currents were normalized by cell capacitance. Peak current density was 56% smaller in hypertrophied NVM (n=22) than in controls (n=23: 10.7 +/- 1.2;C vs. 4.7 +/- 0.8;P pA/pF; p< 0.01) These results suggest that α-adrenergic mediated hypertrophy results in reduced L-type Ca^{2+} channel expression and thus dysfunctional myocardium.

W-AM-D3

STABLE EXPRESSION AND β-ADRENERGIC REGULATION OF A CARDIAC L-TYPE Ca^{2+} CHANNEL. ((M. Wakamori, S. Green*, S. Liggett* and A. Yatani)) Dept. of Pharmacology & Cell Biophysics, *Dept. of Medicine (Pulmonary), Univ. Cincinnati, Cinti., OH 45267.

β-adrenergic agonists regulate cardiac L-type Ca^{2+} channels through cAMP-dependent phosphorylation and direct coupling to G-proteins. However, Ca^{2+} channels expressed in oocytes are not regulated by phosphorylation. Differences may result from the lack of such regulatory components in the oocytes. In order to examine β-adrenergic receptor mediated regulation of cardiac Ca^{2+} channel proteins, we have studied a permanent cell line expressing the cardiac α1, skeletal muscle β and α2 subunits (baby hamster kidney (BHK) cells obtained from Dr. T. Niidome). The expressed current displayed voltage-dependent activation and inactivation, unitary conductance and sensitivity to dihydropyridine drugs characteristic of native cardiac Ca^{2+} channels. Membrane permeable cAMP analogues increased the expressed current. Cells were not responsive to external application of isoproterenol indicating the lack of endogenous β receptors. Transient transfection of the stable BHK cell line with the β1-adrenergic receptor renders the cells responsive to isoproterenol (Fig.). This expression system appears to be well suited for studies of physiological receptor coupled regulatory processes of cardiac Ca^{2+} channels.

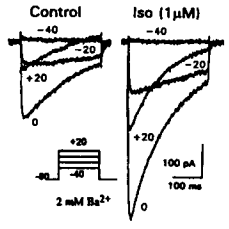

W-AM-D4

REGULATION OF CARDIAC CALCIUM CHANNEL CLONES BY PROTEIN KINASE A. ((J. Costantin*, A. Neely, P. Baldelli, X. Wei, N. Waxham*, L. Birnbaumer and E. Stefani)).*Dept. of Neurobiology and Anatomy, Univ. Texas Med. School, Houston, TX 77225, Dept. of Molec. Physiol. & Biophys., Baylor Col. Med., Houston, TX 77030.

Substantial evidence exists for regulation of native L-type cardiac calcium channels by protein kinase A (PKA). Using on-cell and excised macropatches we have studied the rundown of currents expressed by cardiac calcium channel clone $\Delta N60\alpha_{1C}\beta_2$ (X. Wei, this meeting) in *Xenopus* oocytes. Oocyte membranes are depolarized using a high potassium methanesulfonic bath solution. Pipettes contain 79 mM barium as the charge carrier and also contain 2uM (-)Bay K-8644 to increase channel openings. Complete rundown of single calcium channels upon patch excision into a solution containing no ATP or PKA occurs within 1 minute. Addition of 2mM MgATP to the bath has little effect on the rate of rundown of these currents. Excision of the patch into a solution containing 2mM MgATP and the catalytic subunit of PKA slows or reverses the rundown of these channels for up to 10 minutes. There is no change in the unitary conductance (22 pS) after the addition of PKA. The frequency of long openings increases after excision into PKA as compared to on-cell patches (P. Baldelli, this meeting). Controls are done using identical solutions except that the catalytic subunit of PKA is heat inactivated prior to addition. We are currently testing clones that have alanine substitutions of the serine residues at various consensus sites for PKA on the α_{1C} subunit in an attempt to identify the site or sites responsible for regulation by the catalytic subunit of PKA. (Supported by grants HL37044 to L. B. and AR38970 to E. S. from NIH).

W-AM-D5

DIFFERENTIAL β-ADRENERGIC REGULATION AND PHENOTYPIC MODULATION OF TWO L-TYPE CA CURRENTS IN RAT AORTIC MYOCYTES.

S. Richard, D. Neveu, J. F. Quignard, J. Nargeot (spon. by P. Lorente)
CRBM, CNRS, Route de Mende, BP 5051, 34033 - Montpellier - France.

Adult rat aortic myocytes in primary culture (1-15 days) can express low-voltage-activated (LVA), so-called T-type, and high-voltage-activated (HVA), so-called L-type, Ca^{2+} currents (I_{Ca}). The HVA currents can be subdivided into two distinct patterns referred to as HVA1 and HVA2 and distinguished, using the whole-cell patch clamp technique (18-22 °C), by their voltage-dependent activation/inactivation properties, rate of decay, relative permeability ratio (I_{Ca}/I_{Ba}) and sensitivity to DHP antagonists (Neveu et al., 1993, *Pflügers Archiv*, 424, 45-53). We show here that the two L-type related I_{Ca} are differentially regulated by the β-adrenergic agonist isoproterenol (ISO). For example, ISO at 10 μM increased the HVA2 current (65 ±30 %, n = 10) but had no effect on the HVA1 (neither on the LVA) currents. This potentiation was dose-dependent in the range 0.01-10 μM and was mimicked by the permeant analogue dibutyryl-cyclic AMP (100 μM). Interestingly, the ISO-sensitive HVA2 current was virtually absent in freshly isolated - and well differentiated - myocytes which exclusively expressed HVA1 currents. Both HVA2 and LVA currents appeared after some time in culture, i.e., in correlation with cell dedifferentiation and proliferative activity. The present results are consistent with a phenotypic modulation of the functional expression of two L-type Ca^{2+} channels with distinct electrophysiological and regulatory profiles. They may serve distinct cellular functions involved in the contractile differentiated (HVA1) and the proliferative dedifferentiated (HVA2) phenotypes, respectively.

W-AM-D6

ACETYLCHOLINE ELICITS A DECREASE FOLLOWED BY A REBOUND INCREASE IN Ca^{2+} CURRENT IN CAT ATRIAL MYOCYTES.

((Y.G. Wang and S.L. Lipsius)) Loyola University Medical Center, Dept. Physiology, Maywood, IL 60153 (Spon. by R. Robinson)

A nystatin-perforated patch whole-cell recording method was used to study the effect of acetylcholine (ACh) on Ca^{2+} current (I_{Ca}) in cat atrial cells. K conductances were blocked with external 20 mM cesium (Cs) and replacing K-glutamate with Cs-glutamate in pipette solutions. Holding at -40 and clamping to 0 mV for 200 ms activated control I_{Ca} (trace 1). Exposure to 1 μM ACh for 4 min. significantly decreased peak I_{Ca} from 5.4±0.5 to 3.7±0.3 pA/pF (-31%)(trace 2). Within 30-60 sec. of perfusing ACh-free Tyrode solution, peak I_{Ca} amplitude exhibited a rebound increase to 8.1±0.7 pA/pF (+52%)(trace 3) that returned to control in 3-4 min (trace 4). Exposure to 0.5 mM IBMX increased basal I_{Ca} by 76%. In IBMX, 1 μM ACh failed to decrease I_{Ca} but elicited a significantly larger rebound increase in peak I_{Ca} (15.4±5.4 pA/pF; 97%) compared to control. In 2 μM H-89 (PKA inhibitor) 1 μM ACh decreased I_{Ca} (-38%) but failed to elicit a rebound increase in I_{Ca}. In addition, 0.01 μM ACh decreased I_{Ca} but failed to elicit a rebound increase in I_{Ca}. These results indicate that in atrial cells ACh inhibits basal I_{Ca} and induces a rebound increase in I_{Ca} upon washout. ACh-induced inhibition and rebound of I_{Ca} are not functionally related. ACh-induced rebound of I_{Ca} may be mediated by cAMP-dependent PKA activity.

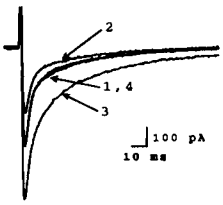

W-AM-D7

CALMODULIN-DEPENDENT PROTEIN KINASE II (CKII) MODULATES LOW VOLTAGE-GATED, T-TYPE, Ca CHANNELS.

((P.Q. Barrett, R.J. Fern, J.J. Nee, H.K. Lu)) Dept of Pharmacology, University of Virginia, Charlottesville, VA. 22908.

In adrenal glomerulosa (AG) cells, the steroidogenic response to low extracellular K (3.5-5 mM) is supported by an elevation of intracellular Ca (Ca_i) that is maintained by the activity of low voltage-gated Ca channels. However, since the Ca channel itself may also be a site of Ca-dependent regulation, we sought to determine if the low-voltage response of T-type Ca channels is modified by the Ca-dependent activation of CKII. Measuring whole-cell currents we show that fixing pipette Ca at 500 nM (+0.2 μM calmodulin (CaM)), increases T-type Ca currents negative to -10mV, shifting the voltage-dependence of activation ($V_{1/2}$) from -15.2 mV (<1nM Ca) to -23.0 mV (500 nM Ca; $p< 0.001$), the latter value similar to that observed with the perforated patch technique. Preincubation with KN-62, which competes with CaM for binding to CKII, abolishes the Ca-induced shift in the $V_{1/2}$ (-14.1 mV; $p<0.002$), while increasing pipette CaM (0.2 to 2.0 μM) reverses this inhibition within 8 min. (-21.9 mV; $p<0.001$). Suprisingly, reducing pipette Ca to 150 nM maintains the shifted $V_{1/2}$ and also facilitates antagonism by a CKII peptide inhibitor (290-309 aa) but not by a PKC peptide inhibitor (19-31 aa). We conclude that the physiologically important low-voltage response of T-type Ca channels in AG cells is in part the result of regulation exerted by CKII.

W-AM-D8

INACTIVATION IN CARDIAC-SKELETAL CALCIUM CHANNEL CHIMERAS.

((L. Parent, M. Gopalakrishnan, A.E. Lacerda and A.M. Brown)) Dept. Molecular Physiology and Biophysics, Baylor College of Medicine, Houston, TX 77030.

The locus for inactivation in calcium channel proteins is unknown. To address this issue, chimeras were constructed between cardiac (H4) and skeletal muscle (Sk4) calcium channel α_1 subunits and expressed *Xenopus* oocytes in the absence of auxiliary subunits. A chimeric construct Sk1H3, in which the first repeat was from skeletal α_1 and the last three were from cardiac α_1 subunit, showed much faster and far more complete inactivation than the wild-type parent H4. With Ba^{2+} ions as the charge carrier, inactivation of Sk1H3 was 90% complete after a 5-s conditioning pulse at +20 mV whereas inactivation of H4 was only 37% complete. Calcium ions increased the extent of steady-state inactivation from 37 to 83% for H4 and from 90 to 95% for Sk1H3. The fast Ba-inactivation was confirmed at the single-channel level; averaged single-channel ensembles showed a 40% time-dependent decline in the mean current during a 320 ms-pulse at +60 mV. We investigated the molecular mechanism of inactivation by examining the role of the N-terminus and the IS5-IS6 linker. Chimera Sk1H3-A, with a cardiac IS5-IS6 linker into the Sk1H3 host, showed fast Ba-inactivation similar to Sk1H3. Chimera Sk1H3-B, with the skeletal N-terminus affixed to H4, inactivated slowly in the presence of barium. Altogether, these results show that inactivation of L-type calcium channels is an intrinsic property of the α_1 subunit and may result from interactions between the four repeats of this subunit. Supported by NIH grant HL37044.

W-AM-D9

MOLECULAR DETERMINANTS OF VOLTAGE DEPENDENT INACTIVATION IN CALCIUM CHANNELS.

((J.F. Zhang, P.T. Ellinor, R.W. Aldrich and R.W. Tsien)) Dept Mol & Cell Physiol, HHMI, Stanford Univ, Stanford, CA 94305

Voltage-dependent inactivation, a fundamental property of Ca channels, helps control Ca entry during repetitive electrical activity. The rate of inactivation varies widely among cloned Ca channel α1 subunits with Ba as the charge carrier, doe-1 being the fastest, BI intermediate and Cardiac L-type (Card) the slowest. To explore the molecular mechanisms underlying the inactivation process, we have constructed chimeric α1 subunits and expressed them with other auxiliary subunits in *Xenopus* oocytes. When the III-IV loop of doe-1 is introduced into BI, there is no significant change in the inactivation rate, despite the large difference between inactivation rates of the wild type channels. In contrast, when the III-IV loop of Card replaces that of BI, the mutant channel inactivates much faster than either parent. Thus, the III-IV loop may not be essential in determining the inactivation rate, whether or not it is involved in the inactivation process. When the first two motifs of BI are replaced with that of doe-1 or Card, the rate of inactivation approaches that of the wild type doe-1 or Card. Additional chimeras allowed us to localize the crucial structural elements to a region that includes IH5, IS6 and the I-II loop. As shown in the figure, the inactivation is about two-fold faster (96.85±7.17 vs 41.31±2.85 ms) when this region of doe-1 is introduced into BI (chimera DB5). Qualitatively similar conclusions were obtained when DB5 was co-expressed with either β1, β2b or β3 subunits. These results reveal key molecular determinants of voltage-dependent inactivation of calcium channels that were not anticipated from previous work on sodium channels.

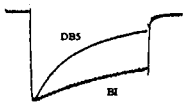

W-AM-D10

Ca-SENSITIVE INACTIVATION OF RECOMBINANT L-TYPE Ca CHANNELS EXPRESSED TRANSIENTLY IN A MAMMALIAN CELL LINE ***((M. de Leon, E. Perez-Reyes, X. Wei, and D.T. Yue))*, *Johns Hopkins Sch. Med., Baltimore, MD 21205***

Ca-sensitive inactivation is a physiologically important feature of L-type Ca channels whereby Ca^{2+} influx speeds inactivation. Cloning and expression of the L-type Ca channel (Mikami *et al*, Nature 340:230), along with genetic manipulation methods, offer the promise of localizing molecular determinants of this property. This approach critically requires an expression system that: lacks contaminating Ca-activated currents (as in oocytes); permits rapid introduction of mutant channel constructs (vs stable cell lines); and provides high-level expression with genuine reconstitution of Ca inactivation. We now find that transient co-expression of CMV-promoter-based constructs carrying the rabbit cardiac Ca channel α_1 and brain/heart β subunits (Perez-Reyes *et al*, JBC 267:1792) in HEK293 cells may satisfy these criteria. Untransfected cells lack appreciable Ca-activated currents or high-threshold Ca channels. In contrast, >30% of transfected cells express dihydropyridine-sensitive currents, with average peak currents ≈450 pA (n=46 cells in 10 mM Ba). Transfection of the α_1 subunit alone yields 3.5-fold lower expression. While Ba^{2+} currents decay <10% by the end of 300 ms steps to +20 mV, substitution of 10 mM Ca as charge carrier yields decays of ≈60% (A,*a*). Classic reconstitution of Ca inactivation is affirmed by the diminished decay at 0 or +60 mV (A, *b&c*, respectively), as if the rate of inactivation parallels Ca^{2+} influx, but not voltage. Elementary and ensemble average currents with 160 mM Ca as charge carrier also demonstrate Ca inactivation (B), and conditional open probability analysis detects "gating plasticity" (Yue *et al*, Science 250:1735), suggesting that the full span of biophysical properties of Ca inactivation is reconstituted. The HEK293 system may prove useful in structure-function studies of the Ca inactivation mechanism.

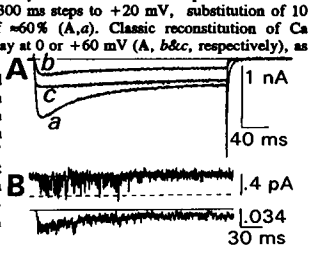

W-AM-E1

SEQUENCE-DEPENDENT TRANSLATIONAL AND ROTATIONAL EFFECTS IN NUCLEIC ACID STRUCTURES. ((Nancy L. Marky and Wilma K. Olson)) Department of Chemistry, Rutgers, the State University of New Jersey, New Brunswick, New Jersey 08903.

The base-to-base virtual bond treatment of DNA used in statistical mechanical calculations of chain properties has been refined by incorporating the six parameters that relate the positions and orientations of sequential bases. The scheme allows for the sequence dependent bending, twisting, and displacement of residues as well as for asymmetry in the angular and translational fluctuations. The new expressions permit, for the first time, examination as a function of chain length of the effects of sequence dependent translations on the average extension, shape, and orientation of nucleic acid molecules. We have examined copolymers made up of alternating B- and A-type helices (kinked structures formed by lateral translations), and intrinsically curved duplexes and their ligand-intercalated complexes. We have calculated a complete set of average configuration-dependent parameters, as well as approximations of the spatial distributions of these molecules. At lengths of 200 base pairs, the curved chains and copolymers with multiple kinks, are more compact on average and are located in a different space from the standard B- or A-DNA helix. While A-DNA is shorter and thicker than B-DNA in X-ray models, the long flexible A-DNA is thinner and more extended on average than its B-DNA counterpart because of more limited fluctuations in local structure. The calculations shed new light on the possible structural role of short A-DNA fragments in long B-type duplexes (*e.g.*, Okazaki fragments). They also offer a model for understanding how GC-specific intercalative ligands can straighten naturally curved DNA. The mechanism is not immediately obvious from current models of DNA curvature, which attribute the bending of the chain to a perturbed structure in repeating tracts of A·T base pairs. (Supported by USPHS grant GM 20861).

W-AM-E2

QUANTITATIVE DESCRIPTION OF DNA SHAPE.

((J.F. Doreleijers, C.-S. Tung, and, D.M. Soumpasis)) LANL, Los Alamos, NM 87544. (Spon. by Byron Goldstein)

We introduce a new general computational scheme for determining the 3D path (curved axis) of an arbitrary DNA structure from its atomic coordinates. It is based on our previous work for extracting the reduced set of conformational parameters from atomic coordinates [1,2] and the approximation of a space curves by means of quintic Bezier curves, in conjuction with an elastic energy minimization criterion for "smoothing". The local DNA curvature and torsion quantitatively measure the shape of DNA structures in geometrically complex situations (e.g. inherently bent DNA, DNA folding and supercoiling, and DNA in DNA-protein complexes.)

[1] C.-S. Tung, D.M. Soumpasis, "A reduced set of coordinates for modeling DNA structures: (III) The construction of DNA helical duplexes along prescribed 3-D curves." in press

[2] D.M. Soumpasis, C.-S. Tung, "A rigorous base pair oriented description of DNA structures", J. of Biomol. Str. and Dyn. 6, 397 (1988)

W-AM-E3

DNA MELTING, PREMELTING AND DYNAMICS MEASURED BY OPTICAL SPECTROSCOPY OF NORMAL AND FLUORESCENT BASES† ((T. M. Nordlund, D. Xu and K.O. Evans)) Dept. of Physics, University of Alabama at Birmingham, Birmingham, AL 35294-1170

Melting, premelting and site-specific thermodynamic transitions are quantitated by temperature-dependent absorption and fluorescence excitation and emission spectra in DNA containing 2-aminopurine (2AP) in place of adenine at site(s) of interest. In d[CTGAATTCAG]$_2$ and d[CTGA(2AP)TTCAG]$_2$, the A→ 2AP replacement depresses the melting temperature but preserves the B-helical conformation and recognition by endonuclease Eco RI. Spectra of the 2AP and normal bases show that when the melting transition is 28 °C, a premelting transition occurs at 10-15 °C. The latter is indicated by a temperature dependent energy-transfer band near 265 nm[1] and by a shift of the excitation spectrum from about 308.5 nm to 306 nm as temperature rises. Premelting is likely connected to a base mobility increase along with increased exposure to a more polar environment. A blue shift of the 2AP absorption spectrum from 315 nm indicates breaking of the 2AP-T hydrogen bond. These measurements suggest that fluorescence comes primarily from stacked, non-H-bonded 2AP bases which sense conformational transitions in the oligomer.

† Supported in part by NSF grant DMB 9118185.

[1] T. M. Nordlund, D. Xu, K. O. Evans, *Biochemistry* (Nov. 23, 1993).

W-AM-E4

EVIDENCE FOR THE FORMATION OF A TRIPLEX VIA A PROTON SWITCH. UV SPECTROSCOPIC AND THERMODYNAMIC IDENTIFICATION OF PROTONATED THIRD STRAND CYTIDINE RESIDUES AT NEUTRALITY IN THE TRIPLEX d(C$^+$-T)$_6$:[d(A-G)$_6$·d(C-T)$_6$].

((L. Lavelle and J. R. Fresco)) Princeton University, Department of Molecular Biology, Princeton, NJ 08544.

Near-UV difference spectral analysis of the triplex formed from d(C-T)$_6$ and d(A-G)$_6$·d(C-T)$_6$ in neutral and acidic solution show that the third strand cytidine residues are protonated at pH 7.0, far above their intrinsic pK_a. Additional support for ion-dipole interactions between the third strand cytidine residues and the G·C target base pairs comes from inverse dependence of triplex stability on ionic strength and strong positive dependence on hydrogen ion concentration. Molecular modeling (AMBER force field) of C:G·C and C$^+$:G·C base triplets with the third strand base bound in the Hoogsteen geometry shows that only the C$^+$:G·C triplet is energetically feasible. Van't Hoff analysis of the melting of triplex and duplex shows that between pH 4.2 - 8.5 in 0.15M NaCl / 0.005M $MgCl_2$ the observed enthalpy of melting (ΔH_{obs}) varies from 5.7 to 8.4 kcal.mol^{-1} for the duplex, and from 7.3 to 9.7 kcal.mol^{-1} for third strand dissociation. Following the approach of Manning, the thermodynamic treatment is extended to allow for separation of experimental variables (Na^+, H^+) in order to determine their contributions to triplex stability. The number of protons released in the dissociation of third strand from duplex at pH 7.0, ΔnH^+, is thereby calculated to be 5.5.

W-AM-E5

THERMODYNAMIC CONTRIBUTION OF THE AA/TT, GA/TC AND GT/AC BASE-PAIR STACKS ON DUPLEX STABILITY

((Karen Alessi and Luis A. Marky))
Department of Chemistry, New York University, New York, NY 10003

We have used a combination of calorimetric and spectroscopic techniques to study the melting behavior of two sets of self-complementary DNA oligomer duplexes with sequences d(GA$_n$T$_n$C) and d(GT$_n$A$_n$C), where n = 4 or 5. In 10 mM phosphate buffer at pH 7, all four molecules melt in two-state monophasic transitions with heats ranging from 73 to 109 kcal-mol^{-1}, T_m's ranging from 47°C to 58°C and average $dT_m/d\log[Na^+]$ values of 14.7°C that correspond to counterion releases of 0.12 (GT$_5$A$_5$C) to 0.16 (GA$_4$T$_4$C). Thus, the addition of two AA/TT base pairs stacks in each set corresponds to an average T_m increase of 6°C resulting from a more favorable enthalpy of 21 kcal-mol^{-1}. The duplexes containing the GA/TC base pair stacks at the ends are more stable by 5°C than the duplexes containing GT/AC at the ends. This is also a result of a more favorable enthalpy of 16 kcal-mol^{-1}, which is 14 kcal-mol^{-1} higher than the predicted value from nearest neighbor interactions. A plausible explanation for this discrepancy is the higher hydration state of the d(GA$_n$T$_n$C) oligomer duplexes. We have probed the overall hydration of these oligomers by investigating calorimetrically the association of netropsin to the minor groove of the A•T stretches of these oligomers. We obtained K_b's of 10^8 M^{-1}, ΔG_b = -11 kcal mol^{-1}, overall binding enthalpies of -1.7 kcal-mol^{-1} for the d(GA$_n$T$_n$C) duplexes and -8.6 kcal-mol^{-1} for the d(GT$_n$A$_n$C) duplexes. These latter results confirm the overall hydration differences in the minor groove of these two sets of oligomer duplexes. This work was supported by NIH Grant GM-42223.

W-AM-E6

WHY CHEMICAL CARCINOGENS BIND SELECTIVELY TO CERTAIN SEQUENCES. ((S.A. Winkle, K. Ferrante, I. Gonzalez, A. Martinez, S. Reinhardt, J. Liang and R.D. Sheardy)) Departments of Chemistry, Florida International University, Miami, FL 33199 and Seton Hall University, South Orange, NJ 07079.

Studies in our laboratory have indicated that the chemical carcinogens N-acetoxy-N-acetyl-2-aminofluorene and 4-nitroquinoline-1-oxide bind very selectively to the sequence motifs T(C/G)TT(G/C) and TC(C/G)TT(G/C). We have synthesized a series of sixteen base pair DNA oligomers containing base permutations on the carcinogen hot spot sequence TCTTGC in their core, e.g, TCTTGC, TCGTGC, TCATGC, TCCTGC. Exonuclease III footprinting, in the absence of carcinogen, of these oligomers indicate a structural distinctiveness, recognizeable by the nuclease, in the carcinogen binding sequence. The presence of the carcinogen binding sequence enhances cleavage by restriction enzymes cutting at sites flanking the carcinogen sequence in the oligomers and in longer DNA fragments. The thermodynamic stabilities of the oligomers have been examined. The oligomer containing the carcinogen site is less stable than the other oligomers. Further, experimental and predicted free energies are comparable for all oligomers other than the oligomer containing the carcinogen site. The carcinogen oligomer is much less stable than predicted. These data suggest that the high affinity of the carcinogen for the sequence TCTTGC is due to structural and thermodynamic distinctiveness of this sequence. (Supported by NIH MBRS GM 08205-07 (SAW))

W-AM-E7

CONFORMATIONS OF SMALL RNA STRUCTURES: RIBOZYMES AND t-RNA. ((Brooke Lustig and Robert L. Jernigan)) Laboratory of Mathematical Biology, National Cancer Institute, National Institutes of Health, Bethesda MD, 20892.

Lattice methods can be used to fully enumerate all chain folds for a number of different stems attached to an internal loop. For a simple cubic lattice there are 36,484,128 lattice chain folds for the sixteen bases enclosing the internal loop of Phe t-RNA. By attaching rigid stems and accounting for their excluded volume these are reduced to only 407,557 configurations. The most common stacking arrangements involve the two pairs of stacked stems as given in the crystal structure. Progressive mutagenesis has shown that the hairpin loops and most of the intermediate stem are not essential for the activity of a hammerhead ribozyme (Lin, N. and Jeang, K.-T., unpublished results). The experiments show that a G remaining on the truncated stem is critical to significant levels of activity. On a cubic lattice, 103,891,782 chain folds are generated for a model system of the ribozyme. For these folds, the critical G is one of the nucleotides most often found near the cleavage site. Among such folds are well stacked structures. A smaller lead ribozyme offers a much smaller number of possible configurations with 561 chain folds. Among these are well stacked configurations.

W-AM-E8

STRUCTURE OF THE SPLICED LEADER RNA FROM *C. elegans*. ((N.L. Greenbaum*, I. Radhakrishnan*, D.I. Hirsh*, and D.J. Patel+)) *Department of Biochemistry and Molecular Biophysics, Columbia University, and +Cellular Biophysics and Biochemistry Program, Sloan Kettering Institute, New York, NY.

Maturation of some mRNAs in nematodes and all mRNAs in trypanosomes involves the addition of a short 5' exon from a spliced leader RNA (SL RNA) to the 3' splice acceptor site of a separate precursor mRNA transcript, a process called trans-splicing. The lowest energy computer-simulated conformation of the 101-nucleotide SL RNA of the nematode *C. elegans* and of other trans-splicing organisms is a structure comprising three stem loops. The proposed first stem loop of the SL1 RNA of *C. elegans* contains both the splice donor site and a complementary base-paired region, analogous with the base-pairing of the 5' splice site of pre-mRNA with the U1 snRNA in cis-splicing. Enzymatic cleavage patterns have shown that the structure of the first 36 nucleotides, predicted to be a loop with a bulged stem, is the same alone as when part of the full-length transcript. A simplification of the original molecule from which the bulged region in the middle of the stem has been deleted was also synthesized. Assignments of NMR spectra have verified the predicted hairpin structure for both molecules and have suggested that the loop might adopt a unique structure. Comparison of spectra of the two molecules has shown that the region surrounding the splice and the loop interactions were unperturbed by deletion of the bulge; therefore, it is unlikely that the loop has tertiary interactions with the bulge region.

W-AM-E9

ACQUISITION OF NATIVE CONFORMATION OF RIBOSOME 23S RNA (L. S Nguyen and K. P. Wong) Department of Biochemistry and Biophysics, University of California, San Francisco, CA 94143

The acquisition of 3-D structure of ribosomal 23S RNA was studied by in vitro reconstitution of 50S subunit from the refolded 23S RNA using circular dichrosim (CD), sedimentation velocity, and two-dimensional gel electrophoresis, and results were compared with those from the native 23S RNA.

A somewhat different mechanism was observed for refolded 23S RNA: a) All 34 proteins from the 50S subunit were found to be associated in normal amounts with the refolded 23S RNA to form the reconstituted intermediates $RI_{50}(1)$, as compared to 21 proteins for native 23S RNA. This $RI_{50}(1)$ particles has a lower s-value (28.2S). b) The first heating at 44°C yielded 3 species with the major species (47.3S), indistinguishable from the native 50S (47.1S), reconstituted 50S from the native (46.7S) and refolded 23S RNA (47.3S). c) As previously observed from native 23S RNA, the increase in Mg (II) to 20 mM shifts the equilibrium in favor of the $RI_{50}(2)$. However, this increase did not eliminate the formation of the heat activitated $RI_{50}*(1)$ (27.1s), indicating a slower transition from $RI_{50}(1)$ to $RI_{50}(2)$, when refolded 23S RNA was used. CD studies showed similar trends of conformational changes during the reconstitution.

These results indicate the refolded 23S RNA has a unique 3-D strucutre that can be recognized and bound by all 34 ribosomal proteins and thus further supported our hypothesis that the 3-D strtucture of this large RNA free-in-solution is determined solely by its ribonucleotide sequence.
(This work was supported by NIH Grants GM 22962 and HL 18905.)

W-AM-E10

PREDICTION OF INTRON AND EXON SEQUENCE IN EUKARYOTIC GENE BY NEURAL NETWORK APPROACH ((Y. Cai, B. Zhou and C. Chen)) Shanghai Res. Cent. of Biotech, Sci Sin. Shanghai 200233, P.R. China

In this paper, a neural network method was applied to predict the splice site location in eukaryotic gene. 90 human glycoprotein genes were used as the samples for prediction. Generally, the predicted splice sites were more than the true splice sites and only a very few nonconsensus splice sites could not be predicted. When the position of the start codon (ATG) and total amount of amino acids were known, the unique sequence of introns and exons could be obtained by computer from numerous possible combinations of predicted splice sites.

BIOPHYSICAL APPROACHES TO TRANSCRIPTIONAL REGULATION

W-AM-SymII-1

SUBUNIT ASSEMBLY IN THE LACTOSE REPRESSOR. ((Kathleen S. Matthews, Jie Chen, Wen-I Chang, and Jeff Nichols)) Department of Biochemistry & Cell Biology, Rice University, Houston, Texas 77251

Mutations that generate monomer or dimer species of the normally homotetrameric *lac* repressor have been identified. Monomeric repressors are unstable, difficult to purify, exhibit no operator DNA affinity, and display inducer binding similar to wild-type tetramer at neutral pH. Dimeric repressors are stable, bind operator with ~50-150-fold lower affinity than tetramer, and are very similar to wild-type protein in inducer binding properties. Dimeric repressors are produced by substitutions or deletions in a C-terminal region containing a leucine heptad repeat, indicative of a coiled-coiled structure. Interruption of this region results in dimers designated "short axis" that presumably have N-terminal helix-turn-turn (HTH) domains aligned in a manner that allows optimal contact with operator. Addition of leucine heptad repeats derived from the GCN4 leucine zipper at the C-terminus does not alter the properties of the tetramer; however, subsequent introduction of a mutation that produces monomeric protein in the wild-type background yields dimeric protein (86 kDa) with an elongated shape: a "long-axis" dimer. Inducer-sensitive DNA binding of this species is reduced ~10^3-fold relative to wild-type, consistent with placement of HTH domains on opposite ends of an elongated dimer. Assembly of the repressor therefore involves at least two separable interfaces. The first connects two short-axis dimers using the leucine heptad repeat region in a possible coiled-coiled structure; strengthening this interface allows generation of the alternate long-axis dimer. The second interface assembles dimers from monomers using regions containing Tyr282 and Lys84, based on behavior of mutant proteins at these sites. These two regions are found on a common face of the monomer in a computer model for core domain of the *lac* repressor. (Supported by NIH grant GM22441 and Welch Grant C-576).

W-AM-SymII-2

Probing the Role of Protein-Protein Interactions in Transcriptional Regulation (Catherine A. Royer, School of Pharmacy, University of Wisconsin-Madison)

Many transcriptional regulators participate in a variety of protein-nucleic acid complexes of different stoichiometries, structures and composition, thereby differentially modulating transcription as a function of cell type or varying physiological conditions. It has thus become increasingly clear that to understand the physical basis of transcriptional regulation, we must characterize the thermodynamics and structural dynamics of the interactions between protein subunits, as well as between proteins and DNA. The *trp* repressor of E. coli, long thought to be a prototypical example of a dimeric DNA binding protein, has been shown to oligomerize both in absence and in presence of operator DNA. We have investigated the interactions between *trp* repressor dimers as a function of solution conditions and the presence or absence of DNA and corepressor using fluorescence-based methodologies. We have observed that repressor dimers oligomerize in solution in the micromolar concentration range to form complexes which are large and polydisperse. These oligomers are destablized by high salt concentration and high pH, implicating an electrostatic component in their association. In addition, the binding of corepressor shifts the equilibrium toward the dimeric form of the protein. Repressor has also been shown to bind to operator DNA as 1:1, 2:1 and higher order complexes in a tryptophan dependent manner. To elucidate the structural basis for the energetic coupling between oligomerization, corepressor binding and interactions with DNA, we have investigated a series of mutant super-repressors with charge change mutations and have found that they fall into particular categories involving perturbations of protein-DNA or protein-protein interactions. Analysis of the available structural information implicates a network of electrostatic interactions in the vicinity of the amino-terminus of the protein. These experiments underscore the importance of probing the solution behavior of transcriptional regulatory systems and demonstrate that such an approach could be quite useful in the investigation of the growing list of eukaryotic transcription factors.

W-AM-SymII-3

USING CHEMICAL PROBE METHODS TO STUDY PROTEIN-DNA COMPLEXES INVOLVED IN TRANSCRIPTION. ((Thomas D. Tullius)) Department of Chemistry, The Johns Hopkins University, Baltimore, MD 21218

"Chemical probe" methods are proving increasingly useful in providing structural and thermodynamic information on complexes of proteins with DNA. I will describe recent work from my laboratory aimed at determining how homeodomain-containing proteins recognize their DNA binding sites. The homeodomain is a sixty amino acid-long sequence that has been highly conserved throughout evolution. These proteins are often involved in specifying developmental pathways. The homeodomain mediates DNA binding through two structural features, a helix-turn-helix that interacts with the major groove of DNA, and an "arm" that binds in the minor groove. Three-dimensional structures of three homeodomain-DNA complexes reveal striking conservation of the interactions between protein and DNA. We are working on three Drosophila homeodomain-containing proteins, ultrabithorax (ubx), deformed (dfd), and engrailed. We are studying ubx and dfd because their "recognition" helices are very similar, yet they function differently in the cell. To compare the structures of these protein-DNA complexes in solution, we are using two chemical probe experiments developed in my lab, hydroxyl radical footprinting and the missing nucleoside experiment. We have found the missing nucleoside experiment, which provides direct information on thermodynamically important contacts between DNA and protein, to have been particularly valuable.

W-AM-SymII-4

REAL-TIME KINETICS OF GENE TRANSCRIPTION: MULTI-COLOR TIME-RESOLVED AND STOPPED-FLOW FLUORESCENCE STUDIES. ((Joseph M. Beechem)) Vanderbilt University, Biophysics, Nashville TN

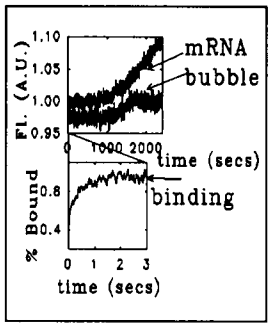

Regulated gene transcription in biological systems involves an extremely complex set of spatial and temporally regulated interactions of multiple proteins with site-specific regions of DNA. Spectroscopic analysis of systems of this type are usually not considered possible. Fluorescence of site-specifically labeled compounds (e.g., DNA, nucleotides, proteins, etc.), however, can be examined in this context. Fluorescence methods also have the distinct advantage of very high sensitivity (pM-nM) and timing resolution (msec). We have assembled four different types of fluorescence spectroscopies, each with a unique excitation/emission wavelength (i.e., "color") capable of simultaneous measurement of: protein/DNA association reactions (anisotropy changes of end-labeled DNA), DNA bending transitions (energy-transfer changes of doubly-labeled DNA), transcription bubble formation (by internal DNA 2-aminopurine probes), and mRNA production (by γ-labeled nucleoside triphosphates). An example of a 3-color measurement of this type is shown in the figure, whereby *E. coli* RNA polymerase first binds DNA (in msec time scale; lower panel), followed by a long-lag, and then instantaneous appearance of a transcription bubble and mRNA.

STRIATED MUSCLE PHYSIOLOGY AND ULTRASTRUCTURE II

W-AM-F1

3-D RECONSTRUCTION OF INSECT FLIGHT MUSCLE BY COMBINATION OF OBLIQUE LONGITUDINAL AND TRANSVERSE SECTIONS.
((Hanspeter Winkler and Kenneth A. Taylor)) Duke University Medical Center, Dept. of Cell Biology, Durham, NC 27707, USA

Oblique section reconstruction (OSR) can produce a 3-D image from a single micrograph of a section through a 2-D or 3-D crystal under certain conditions. Section thickness limits the resolution in a direction perpendicular to the section plane and modulates the 3-D data observed in the image. Section geometry defines the structure factors that can be measured from any one section. These limitations can be overcome by combining sections with different orientations and different thickness which can be done provided that the section thickness is determined. For specimens with low intrinsic symmetry, such as insect flight muscle in the presence of AMPPNP, a new approach to section thickness determination has been developed, which uses a reference constructed by a bootstrap process. In order to recover better the intensity in the outer layer planes, a least squares fitting method has been developed for the deconvolution of section thickness. The combination of oblique transverse and longitudinal section overcomes the limitations on resolution perpendicular to the section plane thereby producing a 3-D image with better resolution than earlier work on muscle in the rigor state could achieve. **Supported by NIH.**

W-AM-F2

ELECTRON MICROSCOPIC RECORDING OF ATP-INDUCED MOVEMENT OF MYOSIN HEADS IN LIVING THICK FILAMENTS. ((H. Sugi, T. Akimoto, N. Oishi, S. Chaen and K. Sutoh*))Department of Physiology, School of Medicine, Teikyo University, Itabashi-ku, Tokyo 173 and College of General Education, University of Tokyo, Meguro-ku, Tokyo 153, Japan.

We have succeeded in recording ATP-induced movement of myosin heads in living thick filaments of rabbit skeletal muscle using a JEOL 2000EXS electron microscope equipped with a gas environmental chamber, in which the filaments were placed between two carbon films with a thin layer of ATP-free solution. Individual myosin heads were marked by attacing colloidal gold particles (diameter 15nm) with antibodies against the junction between 50 K and 23K segments of myosin heavy chain. The image of the filaments was recorded with a Fuji imaging plate system (exposure time 0.1s). To avoid electron beam damage to the filaments, total electron dose was limited to less than 10^{-5}C/cm^2. In ATP-free solution, the position of individual myosin heads, determined with an image processor, did not change appreciably with time. When ATP was applied iontophoretically to the filaments, myosin heads were found to move over a distance of 10-30nm in parallel with the filament axis. As actin is absent in our system, the above ATP-induced myosin head movement is associated with formation of M-ADP-Pi when myosin (M) reacts with ATP. The large myosin head movement strongly suggests that shortening of myosin subfragment-2 is involved in muscle contraction.

W-AM-F3

PRESTEADY STATE ELECTRON MICROSCOPY OF MYOSIN-S1 BINDING TO ACTIN USING A RAPID SPRAY-MIX METHOD. ((Matthew Walker, Howard White, and John Trinick)) Muscle Research Group, Bristol University School of Veterinary Medicine, Langford, Bristol, U.K. and Department of Biochemistry, Eastern Virginia Medical School, Norfolk, Va. 23507.

We have constructed a computer controlled rapid mixing/freezing device to study the structure of presteady state intermediates during the binding of myosin-S1 to actin. Our work is based on a method developed by J. Berriman and N. Unwin (J. Mol. Biol., submitted). A personal computer controls the timing sequence of blotting, spraying, and plunging the samples into liquid ethane. Droplets with an average size of approximately 1 micron containing S1 are sprayed from an atomizer onto a holey carbon grid covered with a solution of f-actin approximately 0.1 micron thick. The grid is then frozen by plunging into liquid ethane. The length of time between spraying and freezing can be varied between 5 and 25 ms by altering the velocity of the grid and the distance traveled between spraying and freezing. Longer delays are obtained by stopping the grid between spraying and freezing. Location of the droplets on the grid is obtained by including ferritin or colloidal gold in the spray. Mixing of the droplets with the solution on the grid is shown to occur in < 5 ms from the observed 5-10 fold dilution of the concentration of the ferritin. We have been able to observe S1 bound to actin after a few milliseconds by this method and are studying the structure of the unstained frozen complex. This work was supported by a grant from the AHA and a Fogarty Senior International Fellowship to HW.

W-AM-F4

TIME-RESOLVED X-RAY DIFFRACTION STUDIES OF MYOSIN HEAD MOVEMENTS IN LIVE FROG SARTORIUS MUSCLE DURING ISOMETRIC AND ISOTONIC CONTRACTIONS ((J. Bordas, G. Diakun, J. Harries, J. Lowy*, G. Mant, M. L. Martin Fernandez, A. Svensson+ and E. Towns-Andrews)) SERC Daresbury Laboratory, Warrington, UK *Open University Research Unit, Boars Hill, Oxford, UK +Physics Department, Leicester University, Leicester, UK (Spon. by C.R. Worthington)

Using synchrotron radiation, the meridional myosin pattern was recorded at 8oC with a time resolution of 2 or 4 ms. During isometric peak tension [Po], 70% or more of the myosin heads diffract with actin-based periodicities, and their axial orientation differs from that at rest. During shortening at a load of ca. 0.27 Po, ca. 85% of the heads [as a fraction of the value at Po], diffract with actin-based periodicities, but their axial orientation does not change from that at rest. During shortening at a negligible load, less than 10% of the heads [as a fraction of the value at Po] diffract with actin-based periodicities, and their axial orientation also remains the same as that at rest. In all cases most of the heads [and/or a major portion of their mass] do not undergo asynchronous axial swinging greater than ca. 0.5 nm about their mean position, which indicates that they do not perform the kind of axial motion required by a tilting head model.

W-AM-F5

INTENSITY CHANGE OF THE 14.5NM AXIAL REFLECTION FROM FROG MUSCLE FIBERS FOLLOWING SHORTENING STEPS OF DIFFERENT AMPLITUDES.

((Gabriella Piazzesi, Vincenzo Lombardi, Hilary Thirlwell[1], Michael A. Ferenczi[1], Ian Dobbie[2] and Malcolm Irving[2])). Dipartimento di Scienze Fisiologiche, Università degli Studi di Firenze, I-50134 Firenze, Italy, [1]National Institute for Medical Research., Mill Hill, London NW7 1AA, U.K., [2]The Randall Institute, King's College London, London WC2B 5RL, U.K.

When a rapid (0.1ms) shortening step of about 6nm/ half sarcomere is imposed on an active muscle fiber the intensity of the 14.5nm x-ray reflection (arising from the axial repeat of myosin heads) decreases with the same time course as the rapid force recovery (Irving et al., *Nature* 357, 156-158, 1992). The x-ray intensity change is larger for larger shortening steps in the range 3-8nm/ half-sarcomere, but there is no significant change for steps of less than 3nm/ half sarcomere, despite the presence of substantial rapid force recovery. Thus the early part of the working stroke in the myosin-actin complex, elicited by filament sliding of less than 3nm, does not change the axial mass distribution. In addition there is no significant change in the inner equatorial reflections, i.e. no change in mass distribution between the filaments. A simple model in which the myosin heads undergo an axial tilt that is symmetrical about the perpendicular to the filament axis following a shortening step of 3nm is consistent with these results.

We thank the non-crystalline diffraction team at the SERC Daresbury Laboratory, Warrington, U.K., where the experiments were carried out, for their assistance. Supported by MRC and NATO.

W-AM-F6

ORIENTATIONAL CHANGES OF RHODAMINE PROBES ON MYOSIN REGULATORY LIGHT CHAINS IN SKINNED MUSCLE FIBERS DURING MECHANICAL TRANSIENTS.

((T.StC. Allen, M. Irving*, and Y.E. Goldman)) Pennsylvania Muscle Institute, University of Pennsylvania, Philadelphia, PA 19104-6085 and *The Randall Institute, King's College London, London WC2B 5RL, U.K.

To examine the relationship between mechanics and angular motions of cross-bridges, we measured tension and fluorescence polarization of acetamidotetramethylrhodamine (ATR) covalently bound to myosin regulatory light chains (RLC) in skeletal muscle fibers during force transients elicited by quick length changes. RLC from chicken gizzard was labelled at Cys-108 using iodo-ATR (Molecular Probes, lot 10A) and exchanged for the native RLC in single rabbit *psoas* fibers. Fluorescence polarization ratios $Q_{\parallel}$ and $Q_{\perp}$ were obtained (60 μs 10-90% instrumental rise-time) using a photoelastic device to modulate the polarization of exciting light (Tanner et al. *J. Mol. Biol.* 223:185-203, 1992). During active contraction at ~30 μM free Ca^{2+}, 11°C, $Q_{\perp}$ = 0.440 ± 0.020, and $Q_{\parallel}$ = 0.353 ± 0.014 (mean ± s.d., n=15). Releases of 6 nm/half-sarcomere, applied as staircases of 5 steps at 50 ms intervals, caused $Q_{\perp}$ to increase transiently by 0.023 ± 0.017 (n=75); $Q_{\parallel}$ changed less. The Fig. shows tension, $Q_{\parallel}$, and $Q_{\perp}$ averaged from 75 steps applied in a total of 15 contractions. The transient increase of $Q_{\perp}$, suggesting rotation of the probes away from the fiber axis, occurred mainly during the rapid force recovery. $Q_{\perp}$ decayed nearly to pre-stretch levels by 50 ms. Similar results were obtained on release during repeated release-restretch perturbations. In contrast, quick stretches led to transient decreases in $Q_{\perp}$ and increases in $Q_{\parallel}$. These results are consistent with tilting motions in the light chain domain of the myosin head in conjunction with force generation, but the signal deflections are smaller than expected if the probes tilt by 45° during quick recovery. Supported by MDA, NIH, and Wellcome Trust, U.K.

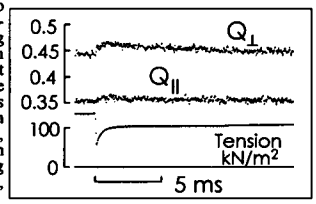

W-AM-F7

PRE-POWER STROKE MYOSIN HEADS ARE DISORDERED AND IMMOBILE - AN EPR STUDY

((D. Raucher and P.G. Fajer, Inst. Molec. Biophysics and Dept. of Biol. Sci., Florida State Univ., Tallahassee, FL 32306))

We have determined the orientation and dynamics of pre-power stroke crossbridges in skinned rabbit psoas fibers. Crossbridges are trapped in the pre-power stroke conformation in the presence of aluminium fluoride, Ca and ATP. Under these conditions spin labeled muscle fibers display 30% of rigor stiffness without generation of force, in agreement with data published for unlabeled fibers [1]. Orientation and dynamics of fibers (labeled with an α- iodoketone derivative of nitroxide synthesized by K. Hideg) were measured with conventional EPR and ST-EPR respectively. In comparison to the relaxed state (disordered heads with microsecond mobility) and rigor (high order and no mobility) we find that in the presence of AlF_4 myosin heads:

(i) are 100% as disordered as in relaxation;

(ii) have intermediate mobility: 30% as rigid as in rigor and 70% mobile as in relaxation.

The correspondence of the immobile fraction (30%) and the stiffness (30%) suggests that the attached heads are immobile yet disordered.

Strongly attached myosin heads at orientations other than in rigor are a candidate for the long sought after state from which head rotation generates force, according to the rotating crossbridge theory [2,3]

[1] Chase B. et al., J. Physiol. 460, p. 231 (1993)
[2] Huxley H.E. Science 164 p. 1356 (1969)
[3] Huxley A.F. and R. Simmons Nature 233, p. 533 (1971)

W-AM-F8

MYOSIN HEADS ARE DISORDERED EARLY IN THE ATPase CYCLE IN SPIN-LABELED RABBIT MUSCLE FIBER BUNDLES.

((Osha Roopnarine and David D. Thomas)) University of Minnesota Medical School, Minneapolis, MN 55455.

We have used **transient EPR spectroscopy, with laser photolysis of caged ATP,** to study the **rate of reorientation** of myosin heads during the **transient phase** of the transition from rigor to relaxation or contraction. We have used an indane dione spin label, designated InVSL, to label cys 707 (SH1) in myosin of rabbit psoas fibers. The spin-labeled myosin heads are well-oriented in rigor, but during steady-state relaxation they are substantially disordered. In steady-state contraction, 79% of the heads are disordered as in relaxation, while the remaining 21% of heads are oriented as in rigor. In relaxation, the transient is biphasic, with rate contants on the order of 50-100 s^{-1} and 10-20 s^{-1}, whereas in contraction only the first (faster) of these phases is observed. The **rapid disordering phase is faster than force generation and probably even faster than the ATP hydrolysis step** for labeled fibers, showing that orientational disordering occurs very early in the ATPase cycle. These results are consistent with a model for force generation in which myosin heads are **highly orientationally disordered in weak-binding states early in the actomyosin ATPase cycle, and become ordered only near the end of the cycle.**

W-AM-F9

FLUORESCENCE POLARIZATION OF ACETAMIDOTETRAMETHYLRHODAMINE (ATR) ISOMERS COVALENTLY BOUND TO SH-1 IN RABBIT *PSOAS* MUSCLE FIBERS FOLLOWING ACTIVATION BY PHOTOLYSIS OF CAGED ATP.

((C.L. Berger, J.S. Craik*, D.R. Trentham*, J.E.T. Corrie* and Y.E. Goldman)) Univ. of Penn., Phila. PA 19104, and *Natl. Inst. for Med. Res., Mill Hill, London NW7 1AA, U.K.

Studies of the orientation of rhodamine probes on SH-1 (Cys-707 of the myosin heavy chain) in single skeletal muscle fibers have demonstrated major probe motions associated with nucleotide binding, but not with force generation (Tanner et al., *J. Mol. Biol.* 223:185-203, 1992). That study however, utilized a commercial sample of dye (Molecular Probes, Inc. lot 9A) which contained unknown proportions of the 5 and 6 isomers. We have therefore synthesized and characterized pure samples of each of the two isomers (U.K. pat. appl. 9320019.4) in order to examine the fluorescence polarization ratios of 5- and 6-ATR covalently bound to SH-1 in single rabbit *psoas* muscle fibers. In rigor, fluorescence polarization ratios were $Q_{\perp} = (_{\parallel}I_{\perp} - _{\parallel}I_{\parallel})/(_{\perp}I_{\perp} + _{\parallel}I_{\parallel}) = 0.633 \pm 0.009$ and $Q_{\parallel} = (_{\parallel}I_{\parallel} - _{\perp}I_{\parallel})/(_{\parallel}I_{\parallel} + _{\perp}I_{\parallel}) = 0.310 \pm 0.009$ for 5-ATR (mean±s.e.m., n=9), and $Q_{\perp} = 0.511 \pm 0.008$ and $Q_{\parallel} = 0.333 \pm 0.009$ for 6-ATR (n=6). During isometric contraction the fluorescence polarization ratios were markedly different: $Q_{\perp} = 0.372 \pm 0.004$ and $Q_{\parallel} = 0.467 \pm 0.008$ for 5-ATR (n=12), and $Q_{\perp} = 0.395 \pm 0.002$ and $Q_{\parallel} = 0.428 \pm 0.002$ for 6-ATR (n=6). The Fig. shows that following the photolysis of caged ATP in the presence of Ca^{2+} at 20°C, 5-ATR probes become disordered and rotate axially well before force development. Similar results were obtained with 6-ATR. These results support the conclusion of Tanner et al. that orientational changes of rhodamine at SH-1 are associated with nucleotide binding rather than force generation. Supported by the MDA, MRC & NIH.

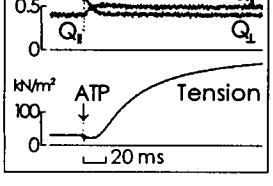

W-AM-F10

ORIENTATION OF ACETAMIDOTETRAMETHYLRHODAMINE (ATR) ISOMERS COVALENTLY BOUND TO REGULATORY LIGHT CHAINS IN RABBIT PSOAS MUSCLE FIBERS.

((Cibele Sabido-David, James S. Craik[1], Birgit Brandmeier[1], John E.T. Corrie[1], David R. Trentham[1], Nick Ling[2] and Malcolm Irving)) The Randall Institute, King's College London, London WC2B 5RL, U.K., [1]National Institute for Medical Research., Mill Hill, London NW7 1AA, U.K., [2]Dept. of Biological Sciences, University of Waikato, Hamilton, New Zealand.

Tetramethylrhodamine derivatives that were specifically substituted in either the 5- or 6- position with an iodoacetamido group* were used to modify cysteine 108 of chicken gizzard regulatory light chain (CGRLC). The fluorescent light chains were exchanged into glycerinated rabbit psoas muscle fibers, and fluorescence polarization ratios parallel ($P_{\parallel}$) and perpendicular ($P_{\perp}$) to the fiber axis were measured in rigor as described previously (*J. Physiol.* **418**:57P. 1989). $P_{\parallel}$ was 0.165 ± 0.027 (mean ± S.D., 8 fibers) for 6-ATR and 0.415 ± 0.015 (n=7) for 5-ATR. The corresponding values for $P_{\perp}$ were 0.566 ± 0.017 and 0.359 ± 0.008. Thus there is a large difference in fluorophore orientation between the two isomers: 6-ATR shows a marked perpendicular orientation preference and 5-ATR shows a slight parallel orientation preference. $P_{\parallel}$ and $P_{\perp}$ values from CGRLC modified with iodo-ATR obtained from Molecular Probes (Eugene, Oregon) were batch-dependent; for example batch 10A gave $P_{\parallel} = 0.180 \pm 0.021$ (n=7) and $P_{\perp} = 0.528 \pm 0.026$, similar to values for 6-ATR, whereas batch 11113 gave $P_{\parallel} = 0.452 \pm 0.031$ (n=3) and $P_{\perp} = 0.319 \pm 0.034$, similar to values for 5-ATR.

* UK Patent application 9320019.4

W-AM-G1

MOLECULAR MECHANISM OF Ca-ATPase REGULATION BY CYCLOPIAZONIC ACID AND HALOTHANE.

((Brad S. Karon, James E. Mahaney, and David D. Thomas)) Dept. of Biochemistry, University of Minnesota Medical School, Minneapolis, MN 55455.

We have studied the effects of cyclopiazonic acid (CPA) and halothane on the enzymatic activity, oligomeric state, and conformational equilibrium of the Ca-ATPase in SR. CPA is a potent inhibitor of Ca-ATPase activity, and this inhibition is competitive with respect to ATP concentration. **Time-resolved phosphorescence anisotropy (TPA)** was used to detect the fraction of Ca-ATPase monomers, dimers, and large aggregates in the absence and presence of CPA. CPA increased the fraction of dimers and large aggregates of the Ca-ATPase. Addition of halothane to SR, or $C_{12}E_8$ solubilization of the Ca-ATPase, increased the apparent K_I of CPA inhibition, and increased the fraction of Ca-ATPase present as monomers. CPA stabilized the E_2 conformation of the Ca-ATPase relative to the E_2-P state, measured by enzyme phosphorylation from inorganic phosphate, and this effect was partially reversed by halothane and $C_{12}E_8$ solubilization. We conclude that **CPA inhibits the Ca-ATPase in part by stabilizing an E_2 dimer form of the enzyme.** This action of CPA is most likely due to competition for a low-affinity ATP binding site on the Ca-ATPase, which in the absence of CPA, is responsible for favoring the transition from E_2 (dimer) to E_1 (monomer).

W-AM-G2

POLYPEPTIDE BINDING TO THE GASTRIC H^+/K^+ ATPASE AND SYNTHETIC FRAGMENTS REPRESENTING THE BINDING REGIONS.

((P.Huang, D.H. Malinowska, M. Clark, K. Blumenthal and J. Cuppoletti)) Dept. Physiol. & Biophys., Univ. of Cinc. Coll. Med., 231 Bethesda Avenue, Cincinnati, OH 45267-0576

The gastric H/K ATPase is inhibited by melittin (*Apis meliffera*) and mastoparan (*Vespula lewissi*). H/K ATPase labeled with [^{125}I]p-azidosalicyl,amido,ethyl,1,3'-dithiopropionylyl melittin or mastoparan was fragmented with V_8 protease. Fragment sequencing indicated that these polypeptides bind to two common regions in the cytoplasmic domain. Thermolysin fragmentation localized one binding region to I_{603}DPPRAT within a 61 amino acid V_8 protease fragment starting at A_{585} and another at Y_{480}RERFP within a V_8 fragment starting at L_{472}. Melittin inhibited K-stimulated ATPase (K-ATPase) non-hyperbolically (n=2) with $K_{0.5}$=0.5 uM, and K-stimulated p-nitrophenyl phosphatase (K-pNPPase) hyperbolically with K_I=0.9 uM. Mastoparan inhibited K-ATPase hyperbolically with K_I=6 uM, but was without effect on K-pNPPase activity. Binding studies indicated two sites for melittin ($K_{0.5}$=0.5 uM, intrinsic K_I=0.2 uM) and a single site for mastoparan (K_I=6 uM). Uniquely, a series of large synthetic polypeptides based on the sequence of the V_8 fragment of the H/K ATPase are also labeled by photaffininity analogs of melittin and mastoparan. These models of the cytoplasmic polypeptide binding region of the H/K ATPase provide a means of deriving structural information regarding the H/K ATPase. Supported by NIH DK43816 and DK43377 (JC and DHM) and NIH training grant HL-07571 (PH). MC is from Schering Corp.

W-AM-G3

IDENTIFICATION OF A POTENTIAL AUTOREGULATORY DOMAIN ON THE GASTRIC H^+/K^+ ATPASE.

((J. Cuppoletti, P. Huang, J.L. VanHeest, M.A. Clark, and D.H. Malinowska)) Dept. Physiol. & Biophys., Univ. of Cinc. Coll. Med., 231 Bethesda Avenue, Cincinnati, OH 45267-0576

The gastric H/K ATPase is inhibited by melittin (*Apis meliffera*) and mastoparan (*Vespula lewissi*). These insectotoxins bind to two sites within the cytoplasmic domain of the alpha subunit of the H/K ATPase. One of these sites is within a 61 amino acid V8 protease fragment starting with A_{585}. The N-terminal region contains the melittin binding region I_{603}DPPRAT and is very hydrophobic. The C-terminal region is similar in structure to melittin. To investigate whether these two regions interact, synthetic polypeptides based on the structure of these regions were tested for effects on the K-stimulated ATPase (K-ATPase) activity. Those peptides with melittin-like C-terminal amino acids inhibited the K-ATPase, and those peptides containing the N-terminal hydrophobic melittin binding region stimulated the K-ATPase. [^{125}I]p-azidosalicyl, amido,ethyl,1,3'-dithio-propionylyl analogs of the peptides labeled the alpha subunit of the H/K ATPase. These results suggest that the regions may interact with each other and form an autoregulatory region in the gastric H/K ATPase. This may be the site of binding of the recently identified parietal cell melittin-like protein which exhibits stimulus dependent association with the H/K ATPase (AJP 264:G637-G644,1993). Supported by NIH DK43816 and DK43377 (JC and DHM) and NIH training grant HL07571 (PH and JLVH). MAC is from Schering Corp.

W-AM-G4

MUTATIONAL ANALYSIS OF THE FIRST EXTRACELLULAR LOOP DOMAIN OF THE YEAST PLASMA MEMBRANE H^+-ATPase

((D. Seto-Young*, S. Na#, B. C. Monk+, J. E. Haber# and D.S. Perlin*)) *The Public Health Research Inst., New York, NY; #Brandeis University, Waltham, MA and +University of Otago, Dunedin, NZ (Spon. by D. Seto-Young)

Transmembrane segments 1 and 2 of the yeast plasma membrane H^+-ATPase are predicted to form a helical hairpin structure that is joined by a short 4 amino acid turn. The hairpin head region (A135-F144) is conformationally active and this region in closely related animal enzymes is believed to be a site for the interaction with clinically important drugs. Genetic analysis shows that it indirectly interacts with the catalytic portion of the enzyme. The hairpin head region was probed using site-directed mutagenesis. Substitution in residues G137-E143 with A gave Hyg B^R except for G137. This phenotype is correlated with a defect in membrane potential. The mutations D143A or N were more severe and gave dominant or recessive lethality. Other mutations L138Y and D140E also produced Hyg B^R. A S139E mutation had no effect. Perturbing the hairpin head region by inserting the extra amino acids G, A, and S between L138 and S139 gave Hyg B^R of varying severity. Addition of T or AA residues was not tolerated. In most cases, the mutant enzymes showed altered kinetics for ATP hydrolysis and proton transport. These results support the notion that transmembrane segments 1 and 2 and the linking hairpin head region form a conformationally sensitive region that is coupled to the catalytic ATP hydrolysis domain.

W-AM-G5

INTERACTION OF OUABAIN WITH RAT α2 AND α3 ISOZYMES AND WITH MUTANTS OF SHEEP α1 NA^+,K^+-ATPASE.

((E.T. Wallick, C.L. Johnson, J.B. Lingrel, W.J. O'Brien, and P.J. Schultheis)) University of Cincinnati College of Medicine, Cincinnati, OH 45267-0575 (Spon. by T.L. Kirley)

Measurement of rates of association and dissociation in the presence of Mg^{2+} plus P_i have been used to characterize the binding of ouabain to Na^+,K^+-ATPase. Kinetic analysis of enzyme prepared from rat brain indicated that the 3 isozymes were present in ca. equal amounts in this tissue. The α2 isozyme had a faster off rate than α3, resulting in a 13-fold higher ouabain affinity for the α3 isoform. cDNA's encoding for the rat α2 and α3 were separately transfected into NIH 3T3 cells. Analysis of membranes isolated from these cells confirmed the data obtained from the tissue study. Mutation of Arg 880 to Pro (R880P) in sheep α1 Na^+,K^+-ATPase causes a 10-fold increase in off rate and a 2-fold increase in on rate, suggesting that the H7-H8 extracellular loop comprises a portion of the ouabain binding site. Mutants C104A, Y108A, E116Q, P118K and Y124F have 1-4 fold faster off rates than wild type. In addition, P118K has a 2-fold slower on rate, suggesting that the H1-H2 domain may participate directly in ouabain binding as well as be involved in conformational changes. K^+ inhibits the rate of binding of ouabain to wild type Na^+,K^+-ATPase with a K_D of 1 mM. None of the mutations above affected the affinity for this K^+ site. Supported by NIH Grants HL 50613, HL 28573 and HL 41496.

W-AM-G6

TOPOLOGICAL MODELS OF THE ALPHA CHAIN OF Na/K-ATPase BASED ON PROTEOLYSIS AT THE EXTRACELLULAR SURFACE.

((R.Goldshleger and S.J.D.Karlish)) Biochemistry Dept. Weizmann Inst. of Science, Rehovoth 76100, ISRAEL.

Models of topological organization of the α-chain of Na/K-ATPase have been proposed, on the basis of hydropathy analysis, but direct determination of topology is essential. It is now accepted that both N- and C-terminals are cytoplasmic, indicating the existence of an even number of trans-membrane segments, but hydropathy analysis is ambiguous, particularly in the C-terminal region, and it is uncertain whether there are 10 or only 8 segments and where they are located in the primary sequence. The work described here utilises proteolytic digestion of renal Na/K-ATPase in well defined membrane vesicles. Recently we have shown that the N-terminal residue Asn^{831} of a C-terminal 19kDa fragment of the α-chain is located on the cytoplasmic surface (Goldshleger et al 1993 J.Biol.Chem 268:4371), indicating the existence of two trans-membrane segments M5+6 between the large cytoplasmic loop and Asn^{831}. The question arises whether there are 4 or only 2 segments in the 19kDa fragment. The α-chain is resistant to proteolysis at the extracellular surface, but digestion by trypsin and chymotrypsin has now been demonstrated with right-side-out renal vesicles. This requires heating of the vesicles to 55°C for 30 min, before cooling to 20°C and proteolysing. The α-chain is cut to a fragment of apparent M_r 91kDa. In Rb-loaded vesicles the α-chain is protected. The heating inactivates ATPase activity and Rb occlusion, in the Rb-free but not in the Rb-loaded vesicles. The N-terminal of the 91kDa fragment is Gly^1, and therefore the split(s) occurred near the C-terminal. Immunoblots of SDS-PAGE of digested membranes, using an antibody against the C-terminal tetrapeptide ETYY, reveal four tryptic or chymotryptic fragments with M_r 14.5,12.1, 9.9 and 7.4kDa or M_r 15.7, 13.1, 9.6 and 7.8 kDa, respectively. The N-terminal of the 14.5kDa tryptic fragment has been identified as Trp^{887}. These findings are discussed within the framework of topological models of the α-chain with 8 or 10 trans-membrane segments respectively.

W-AM-G7

IDENTIFICATION OF AMINO ACIDS IN THE ATP BINDING SITE OF NA^+/K^+-ATPASE AFTER LABELING WITH AZIDO NUCLEOTIDES.

((C.M. Tran, E.E. Huston, and R.A. Farley)) University of Southern California School of Medicine, Los Angeles, CA 90033

The active transport of Na^+ and K^+ by Na^+/K^+-ATPase (NKA) requires the hydrolysis of ATP by the protein. 2-N_3-ATP and 8-N_3-ATP are also utilized by NKA as substrates, and in these experiments, both 2-N_3-ATP and 8-N_3-ATP have been used to covalently label the ATP binding site of NKA after illumination with UV light. ATP hydrolysis by NKA was inhibited up to about 50% by both azido nucleotides after photolysis, and inhibition was prevented by the presence of 0.1-0.2 mM ATP. In both instances, the extent of ATP-protectable inhibition was linearly correlated with the stoichiometry of ATP-protectable incorporation of the probe into the α subunit of NKA. The extrapolated stoichiometry of incorporation of 2-N_3-ATP into the protein at 100% inhibition was the same as the ATP-binding capacity of the enzyme, however, because the linkage between 8-N_3-ATP and NKA was unstable, the extrapolated stoichiometry was lower for this probe. A large protease-resistant fragment of 30 kDa containing 2-N_3-ATP was seen after trypsin digestion of labeled NKA, and denaturation with urea was required in order to digest this fragment further. The amino acid sequence of the 2-N_3-ATP-labeled peptide corresponds to amino acids H496-R510 of the NKA α subunit. G502 was absent from this sequence, indicating that this amino acid is labeled by 2-N_3-ATP. The amino acid sequence of the 8-N_3-ATP-labeled peptide corresponds to residues 470-495 of the NKA α subunit. The labeled amino acid was identified as K480. (Supported by GM28673 and AHA-GLAA)

W-AM-G8

SEQUENTIAL POTASSIUM BINDING IN THE E_2-P CONFORMATION OF THE Na,K-PUMP.

((R. Bühler and H.-J. Apell)) Dept. of Biology, University of Konstanz, D-78434 Konstanz, Germany.

Ion binding to the Na,K-ATPase from the extracellular medium has been shown to be electrogenic. Due to this fact ion binding or release can be monitored in purified membrane fragments with a high density of pumps by the styryl dye RH 421. This fluorescent probe responds to changes of the local electric field produced by ion movements into or out of the binding sites.

The fluorescence decrease observed during the electrogenic partial reaction P-$E_2 \rightarrow$ P-$E_2K \rightarrow$ P-E_2K_2 is about 60%. Gradual binding can be measured with high accuracy by titration of the fluorescence amplitude with increasing K^+ concentration. A Hill plot of the K^+ binding resulted in an apparent half saturation constant of 0.2 mM and a Hill coefficient of 1.33 at 20 °C, indicating a slightly cooperative effect in the binding of 2 K^+ ions. Assuming sequential binding a mathematical model can be formulated which allows to fit the titration curves with equilibrium dissociation constants of both binding sites, K_1 and K_2.

These parameters and the half saturating concentration of K^+, $c_{1/2}$, have been determined in the temperature range between 10 °C and 35 °C. They differ at low temperatures: K_1 = 0.24 mM, K_2 = 0.09 mM (10 °C) and merge at temperatures above 20 °C: $K_1 = K_2$ = 0.3 mM (35 °C). The half saturation concentration, $c_{1/2}$, increases from 0.14 mM (10 °C) to 0.3 mM (35 °C) with an activation energy of 21.9 kJ/mol.

W-AM-G9

THE SODIUM PUMP AT 200 kHz.

((D.W. Hilgemann)) Department of Physiology, University ot Texas Southwestern, Dallas, TX, 75235.

Ion binding reactions may be important electrical events in the function of ion transporters and pumps, possibly analogous physically to the gating of some ion channels by the binding of impermeant ions. Here I describe measurements of extracellular Na binding by the Na/K pump in giant membrane patches from guinea pig myocytes at a resolution of 4 μs and 50 charges per μm^2. Na/K pump charge movements are monitored directly as charge transfer, the time integral of membrane current, subtracting baseline records from records in the presence of both cytoplasmic Na and ATP. 'Slow' signal components predominate the charge transfer records. They increase monotonically in rate from a minimum of ~400 s^{-1} at positive potentials to a maximum of ~5000 s^{-1} at -250 mV (37°C). Fast charge movements, complete within 4 μs, precede the slow components. The fast components are abolished by hyperpolarizing prepulses, by removal of extracellular Na, and by extracellular ouabain; they are evidently enhanced when pump cycling is prevented. All charge movements can be accounted for assuming that fast Na binding reactions are the exclusive source of Na/K pump electrogenicity. Slow charge movements then arise from voltage-independent processes in equilibrium with the ion binding reactions. The entire Na^+ release process can be modelled as a stepwise 'opening' of binding sites which shifts membrane field simultaneously across the (negatively charged) binding sites and Na^+.

W-AM-G10

ABSORPTION OF FREE ENERGY FROM FLUCTUATING ELECTRIC FIELDS BY A MEMBRANE ION PUMP TO PERFORM CHEMICAL WORK.

((T.Y. Tsong[1,2], T.D. Xie[2], P. Marszalek[2] and Y.D. Chen[1,3])) Dept. of Biochem., [1]Hong Kong Univ. of Sci. & Tech., [2]Univ. of Minn., and [3]NIDDKD, NIH.

A random-telegraph fluctuating electric field (RTF) consisting of alternating square electric pulses with random lifetimes was found to stimulate the Rb^+-pumping mode of the Na,K-ATPase of human erythrocytes (RBC). A random number generator produced a chain of triggering signals in a PC, which was then used to drive a 50 MHz functional generator to obtain an RTF of a desired mean frequency and frequency distribution. The net RTF stimulated, ouabain sensitive Rb^+ influx of RBC was monitored with $^{86}Rb^+$. Consistent with the previous experiments using the sinusoidal electric fields for stimulation, the RTF induced Rb^+ pumping exhibited an amplitude optimum at 20 V/cm and a frequency optimum at 1.0 kHz. At 4°C, the maximal stimulated activity under these optimal conditions was approx. 25 / RBC-hr, which is about 50% higher than that obtained with the sinusoidal electric field. Analysis based on theory of electroconformational coupling (ECC) was performed for a four state ion transport model to derive the rate constants for each kinetic step. The advantage of using the RTF for study are, first, an analytical solution can be derived for any kinetic model based on the ECC using the diagram methods, and second, an RTF can more realistically mimic the local electric potential of a transmembrane enzyme than can a sinusoidal field. Our results indicate that Na,K-ATPase can recognize an electric signal, with high fidelity, for energy coupling, and that ECC is a plausible mechanism for cellular transduction of electric signals. References: DS Liu et al. J. Biol. Chem. 265, 7260, 1990; RD Astumian et al. Proc. Natl. Acad. Sci., 84, 434, 1987; YD Chen, Proc. Natl. Acad. Sci., 84, 729, 1987; TY Tsong, Biochim. Biophys. Acta 1113, 53, 1992.

SPECTROSCOPY

W-AM-H1

^{13}C-^1H SPIN-COUPLING CONSTANTS IN OLIGONUCLEOTIDES: POTENTIAL OF $^1J_{CH}$, $^2J_{CH}$ and $^3J_{CH}$ AS CONFORMATIONAL PROBES.

((Anthony S. Serianni, Paul B. Bondo, Carol A. Podlasek, Wayne A. Stripe and Timothy J. Church)) Department of Chemistry and Biochemistry, University of Notre Dame, Notre Dame, IN 46556.

Three-bond ^1H-^1H spin-coupling constants ($^3J_{HH}$) are commonly used to evaluate the solution conformations of furanose rings, either as free entities or as components of more complex biomolecules (e.g., oligonucleotides). The well known flexibility of these rings, while probably important in mediating biological recognition, nevertheless complicates the interpretation of $^3J_{HH}$. As a consequence, it is desirable to access other NMR parameters to assist in conformational analysis. We are studying one-, two- and three-bond ^{13}C-^1H spin-couplings in β-D-ribofuranosyl and 2-deoxy-β-D-ribofuranosyl rings using a combination of experimental and computational approaches. Specifically, we have measured ^{13}C-^1H couplings via 1-D and 2-D NMR methods in a series of ^{13}C-labeled carbohydrates that contain fixed-geometry C-H coupling pathways mimicking those found in discrete furanose ring conformers. These data are supplemented by *ab initio* molecular orbital calculations (MP2/6-31G* basis set) on a deoxyfuranose model as a means to evaluate structural parameters affecting J_{CH}. Preliminary results indicate that C-H bond lengths, substitution patterns and/or dihedral angles affect coupling magnitudes and signs. When used in concert, $^1J_{CH}$, $^2J_{CH}$ and $^3J_{CH}$ should provide valuable new information on furanose ring conformation and dynamics in oligonucleotides.

W-AM-H2

PROTEIN ACTIVITY EFFECTS ON THE HYDRATION OF 7S AND 11S SOY GLOBULINS DETERMINED BY ^{17}O NMR RELAXATION.

((I.C. Baianu, T.C. Wei, and E.M. Ozu)) AFC-NMR Facility, University of Illinois at Urbana, Urbana, IL 61801-3852. (Spon. by H. Pessen).

The molecular basis of purified soy protein fraction functionalities was investigated in aqueous solutions with added salt. Our high-field ^{17}O nuclear magnetic resonance (NMR) results on soy globulin hydration and soy protein interactions at high ionic strengths indicate that protein activity has a marked effect on the rheological, aggregation and hydration properties of 7S and 11S soy globulins. Nonlinear regression analysis of ^{17}O NMR data for 7S and 11S soy globulins at pD 7.6 in phosphate buffer containing 0.4 M NaCl allowed us to determine both the hydration and the second order virial coefficient B_ϕ of protein activity for the 7S and 11S fractions. Under these conditions of pH and high ionic strength the value of B_ϕ for 7S and 11S was negative (-1.2), indicating the presence of globulin self-association, whereas the hydration of self-associating 11S particles was about 30% higher than that of 7S. The value of the apparent correlation time for the water hydrating these soy globulins was about 40 ps at 20°C and pD 7.6, with 0.4 M added NaCl. Specific anion and cation effects on salting-in and salting-out of soy globulins were monitored by NMR, and follow the lyotropic series. Such effects can be understood with a thermodynamic model that links protein solubility to Gibbs free energy of salt binding, as in Wyman's theory of linked functions.

W-AM-H3

Differences in Phosphate Metabolites in Cells of Neuronal and Glial Origin - 31P NMR Spectroscopic study. Archana Singh and Nanda B. Joshi, Department of Biophysics, National Institute of Mental Health and Neuro Sciences, Bangalore-560 029,(India)

31P NMR Spectroscopy was used to monitor the phosphate metabolites in established cell lines of glial (U-87 MG) and neuronal origin (PC12). The cultured cells were embedded in agarose gel threads and perfused with a balanced salt solution. The 31P NMR spectrum of PC12 cells showed resonances arising from ATP, PCr, Pi, PME and PDE. The 31P NMR spectrum of U-87 MG cells, on the other hand, showed resonances from ATP, Pi, PME and DPDE. PCr and PDE peaks were found to be absent in U-87 MG cells. Experiments performed in the presence of metabolic inhibitors suggest that in PC12 cells both glycolysis and oxidative phosphorylation pathways contribute to ATP production, whereas oxidative phosphorylation was found to be the major ATP producing pathway in U-87 MG cells. These cells were found to possess energy reserves in the form of glycogen as evidenced by the presence of the DPDE resonance. The difference observed in the energy metabolic pathways of PC12 and U-87 MG cells may be related to the energy requirements for their function.

W-AM-H4

SOLID-STATE NMR OF MAGNESIUM-25 BOUND TO DNA ((Raju Subramanian, Jennifer Jerlstrom, William H. Braunlin, and Gerard S. Harbison)) University of Nebraska-Lincoln, Department of Chemistry, Lincoln, NE 68588-0304.

^{25}Mg is a spin 5/2 nucleus with a natural abundance of 10.13% and a low NMR frequency (18.4 MHz at 7 Tesla field). It also a relatively large quadrupole moment: quadrupole coupling constants for ^{25}Mg in the few crystalline systems studied range from 1 – 4 MHz. For these reasons, until now, solid-state ^{25}Mg NMR has not previously been applied to macromolecular biological systems.

Using isotope-enriched material, we have measured for the first time the solid-state NMR spectrum of ^{25}Mg bound to calf-thymus DNA. For DNA samples with relatively low magnesium loading (less than 1 mol/mol base pairs), at 75% humidity, we observe a central (–1/2 — +1/2) NMR transition several kilohertz broad. Using a modified quadrupolar echo sequence we can also detect the ±1/2 — ±3/2 transitions, which form a Pake doublet with a splitting of approximately 330 KHz. This leads to a quadrupolar coupling constant somewhat in excess of 1 MHz, sufficiently large for the broadening of the central transition to be ascribed to second-order quadrupole effects. The quadrupolar coupling constants determined directly by solid-state NMR are in excellent agreement with previous determinations using liquid state relaxation techniques.

W-AM-H5

ALTERNATIVES FOR KAPPA-SQUARED CONTOUR PLOTS ((B.Wieb Van Der Meer, Sun-Yung Chen and Steven K. Boddeker)) Department of Physics and Astronomy, Western Kentucky University, Bowling Green, KY 42101

Dale *et al.* (Biophys.J. 26, 161-194, 1979) presented kappa-squared contour plots to find the minimum and maximum value for the orientation factor (kappa-squared) as a function of depolarization factors for the Donor ($\langle d_D^x \rangle$), for the Acceptor ($\langle d_A^x \rangle$), and for transfer (d_T^x). We present alternatives based on deriving these extrema analytically. There are two cases: 1. d_T^x is not known, 2. d_T^x is known. For the first case we have derived a map of the $\langle d_D^x \rangle$-$\langle d_A^x \rangle$ plane with regions where the maxima and minima can be specified with equations. For the second case we have a recipe that allows one to find accurate values of the minima and maxima for all possible parameter values. This work is supported by the National Science Foundation EPSCoR program (EHR-9108764). We will also present a "sneak preview" of a book *Resonance Energy Transfer: Theory and Data* by B.W. Van Der Meer, G. Coker III and S.-Y. Chen, to be published by VCH publishers.

W-AM-H6

QUENCHING OF FLUORESCENCE BY LIGHT; A NEW METHOD TO CONTROL THE EXCITED STATE LIFETIMES AND ORIENTATIONS OF FLUOROPHORES. ((Ignacy Gryczynski, Józef Kuśba, Valery Bogdanov*, and J.R. Lakowicz)) University of Maryland, School of Medicine, Center for Fluorescence Spectroscopy, Department of Biological Chemistry, 108 N. Greene Street, Baltimore, MD 21201; *Vavilov State Optical Institute, Birzhevya linya, 14, 199034, St. Petersburg, Russia (Sponsored by H. Malak)

We report the first time-resolved studies of quenching of fluorescence by light i.e., "light quenching." The dyes 4-(dicyanomethylene-2-methyl-6-(p-dimethamino)-4H-pyrane (DCM) and Rhodamine B (RhB) were excited in the anti-Stokes region from 560 - 615 nm. At high illumination power the intensities of DCM and RhB were sub-linear with incident power, an effect we believe is due to stimulated emission and not ground state depopulation. The extent of light quenching was proportional to the amplitude of the emission spectrum at the incident wavelength, as expected for light-stimulated decay from the excited state.

Light quenching of fluorescence provides a new method to control the excited state population and orientation of fluorophores. Light quenching can be used to break the Z-axis symmetry which is present in most experiments, and to change the polarization over a wide range -1.0 to +1.0. Also, the extent of light quenching can be expected to depend on the solvent relaxation time (τ_R) and the rotational correlation time (θ), and the extent to which these processes occur within the width of the quenching pulse. For excitation and quenching by a single pulse of width t_p, more light quenching is expected for $\tau_R > t_p$ because the emission spectrum has not yet relaxed from overlap with the quenching wavelength. In conclusion, light quenching has numerous potential applications for studies of the dynamics of fluorescent substances.

W-AM-H7

IMPROVED FLUORESCENCE ENERGY TRANSFER USING LANTHANIDE CHELATES.
((P.R. Selvin, M.P. Klein and J.E. Hearst)) Calvin laboratory and Department of Chemistry, University of California, Berkeley and Lawrence Berkeley Laboratory, Berkeley CA 94720.

We have developed a fluorescence energy transfer technique in which the donor is a luminescent terbium chelate and the acceptor is a standard organic dye. The donor has a millisecond lifetime and isotropic emission, making lifetime measurements relatively simple and significantly minimizing uncertainty in the orientation-dependence (κ^2) of energy transfer. In addition, using both spectral and time discrimination, the sensitized emission of the acceptor can be measured with no interfering fluorescence. This is in contrast to standard dye-pairs, where the sensitized emission is typically on-the-order of the background. We have achieved a signal to background (where background is determined primarily by detector noise) of several hundred on an 8-mer DNA duplex labeled on 5' ends with donor and acceptor (donor and acceptor separated by approximately 37Å). We find the fraction of energy transfer to be 85%. We also report the first measurement of the acceptor's sensitized emission lifetime. This measurement is completely insensitive to concentration and to incomplete labeling — only the donor-acceptor complex contributes to this signal. Spectroscopic and chemical characterization of the chelate (which can also be used with europium, another potentially interesting donor) will be presented. This work supported by NIH grant FD 8R1 GM 41911A-03-NF-03/92.

W-AM-H8

CHARACTERISTICS OF A MICRO-STOPPED FLOW APPARATUS. George Czerlinski, Michael Isaacson, Richard Ramires, Shu Chen, and Linda Powers, National Center for the Design of Molecular Function, Logan, UT 84322-4630.

A small stopped flow apparatus was designed and built using Hamilton gastight syringes and Hamilton valves. A fiberoptic light pipe transfers light between the light source (a tungsten iodine lamp) and a multiplier phototube (RCA 6342A) via the observation cell. Dielectric interference filters are used to obtain monochromatic light. The light path length in the flow tube is 10 mm resulting in a time resolution of 1 msec at a flow velocity of 10 m/sec. The diameter of the cylindrical light path is 1 mm, giving a filling volume of 8 µl. The mixing ratio from the two 250 µl syringes is 1:1. The minimum usable volume is 10 µl/syringe. A linear stepping motor (Compumotor LX-20) is used to drive both syringes simultaneously. A special acceleration profile has been incorporated to effect smooth acceleration to 10 m/sec flow velocity. The same profile is used for decelleration. A peak acceleration of 8 G was employed. Online data evaluation is incorporated allowing exponential and numerical evaluation of kinetic data. Feasability is shown using the reaction of horse heart ferrocytochrome *c* with ferrihexacyanide, observing changes at 550 nm. A rate constant was obtained which corrsponds to the results obtained before by Brandt et al (J. Biol. Chem. 241, 4180). This flow apparatus has also been effectively used with a dual beam spectrophotometer following selected reactions of peroxidases (Yamazaki et al, in prep.).

W-AM-H9

CHARACTERIZATION AND MANIPULATION OF CELLS USING A. C. ELECTRICAL FIELDS. ((P.R.C. Gascoyne, Y. Huang, X-B. Wang and F.F. Becker)) University of Texas M. D. Anderson Cancer Center, Department of Molecular Pathology, Box 89, 1515 Holcombe Boulevard, Houston, TX, 77030, USA

An overview of A. C. electric field induced pondermotive effects, including dielectrophoresis (DEP), electrorotation (ROT) and travelling-wave dielectrophoresis (TWD), on biological cells will be presented when they are subjected to (i) non-uniform AC electric fields, (ii) rotating fields, and (iii) travelling electric fields. These phenomena are closely related through the induced dipole moment and are strongly dependent on cell dielectric properties.

The measurements of DEP, ROT and TWD frequency spectra allows the investigation of cell surface charge, cell membrane morphology and of the dielectric properties of the cytoplasm and its organelles. Examples will be given showing how these spectra reflect the subtle cell physico-chemical differences occured due to differing cell type and cell physiological states.

An understanding of these effects has been made possible by novel microelectrode designs. These designs may permit biomedical and biotechnological applications of these phenomena, including cell manipulation, concentration and cell separation. Examples will be shown for various cell types, including murine erythroleukemia cells, in a short video presentation.

W-AM-H10

THERMAL UNFOLDING OF HUMAN AND BOVINE ALBUMINS AND THEIR ADHESION AT A SOLID/LIQUID INTERFACE. ((R. Nicholov and F.DiCosmo)) Centre for Plant Biotechnology, Dept. of Botany; Institute of Biomedical Engineering, University of Toronto, 25 Willcocks Str., Toronto, Ont.M5S 3B2

HSA and BSA were labelled with maleimido- and amino proxyl spin labels. Thermal unfolding of proteins was recorded using ESR and fluorescence spectroscopy and the adhesion of proteins at the solid/liquid interface at different temperatures (10°-78°C) was studied. The data show that the inflection points of Arrhenius plots of ESR parameters are in excellent agreement with the inflection points of adsorption curves. The immobilization of the spin labels due to the adsorption of protein at the solid surface induced changes in hyperfine line splitting and rotational correlation time of ESR spectra indicating the conformational changes of the proteins. These changes were mimicked by thermally induced changes of ESR spectral characteristics at low temperatures. The ESR spectrum of adsorbed HSA at the solid surface resembles the spectrum of spin labelled HSA in liquid recorded at -58 ° C. The adsorption of spin labelled proteins to the surface of phospholipid liposomes did not cause any additional immobilisation of the spin labels.

MODULATION OF CHANNELS

W-AM-I1

NITRIC OXIDE DIRECTLY ACTIVATES CALCIUM-DEPENDENT POTASSIUM CHANNELS IN VASCULAR SMOOTH MUSCLE CELLS
((V.M. Bolotina, J.J. Palacino, P.J. Pagano and R.A. Cohen))
Boston University Medical Center, Boston, MA 02118, U.S.A.

Here we present evidence that both exogenous nitric oxide (NO) and naturally produced endothelium-derived relaxing factor (EDRF) directly activate single Ca^{2+}-dependent K^+ channels (K^+_{Ca}) in excised membrane patches from rabbit aortic smooth muscle cells. Channel activation by NO occurred rapidly in cell-free membrane patches without requiring cGMP and ATP. The effect of NO (0.2-5μM) was transient, the duration and magnitude depending on concentration. NO increased the open channel probability when applied from either side of the membrane, and caused the appearance of long bursts of channel openings (up to 20 s) preceded occasionally by 1-10 s periods of channel closure. Activation of channels by NO was shown to be dependent on nitrosylation of sulfhydryl groups, being completely prevented by prior modification of these protein constituents with n-ethyl-maleimide (NEM). NO did not affect single channel conductance. Naturally produced EDRF also activated K^+_{Ca} channels directly, as was shown by exposure of outside-out membrane patches to perfusate coming from a rabbit aorta before and during endothelial cell activation by acetylcholine. These studies demonstrate a novel direct action of NO on single K^+_{Ca} channels which is different from the well established cGMP-dependent pathway. This is a new mechanism of K^+_{Ca} channel modulation through modification of protein sulfhydryl groups.

W-AM-I2

NITRIC OXIDE MODULATES CHOLINERGIC SLOWING OF HEART RATE.
((Y. Shimoni, X. Han, W.R. Giles)) Medical Physiology, University of Calgary

Acetylcholine (ACh) slows heart rate by altering several different transmembrane ionic currents. One of these changes is an inhibition of L-type calcium current, I_{Ca}, under both control conditions, and after I_{Ca} has been increased by a β-adrenergic agonist. Our data were obtained from single sinoatrial node cells using the whole-cell patch clamp method. In the presence of a β-adrenergic agonist, inhibition of the NO generating enzyme, NO synthase (NOS), by preincubation of cells in 1 mM L-Nitro-arginine methyl ester (L-NAME) abolishes the effect on I_{Ca} of the muscarinic cholinergic agonist carbachol (CCh). In contrast the CCh-dependent background potassium current is unaffected. Co-incubating cells in L-NAME and arginine (the endogenous substrate of NOS) restores the inhibitory effect of CCh on I_{Ca}, thus ruling out a direct effect of L-NAME on muscarinic receptors. The NO-generating drug, SIN-1, also attenuates I_{Ca} in the presence of β-adrenergic stimulation. In combination, these results demonstrate that NO is an obligatory mediator in the autonomic regulation of the heart rate.

Supported by the Canadian Medical Research Council and Heart Foundation.

W-AM-I3

A NITRIC OXIDE DONOR HAS STIMULATORY AND INHIBITORY EFFECTS ON THE CARDIAC CALCIUM CURRENT, BOTH OF WHICH ARE INHIBITED BY A G-KINASE BLOCKER ((Susanne J. Dollinger & Gordon M. Wahler)). Dept. of Physiology & Biophysics, Univ. of Illinois, Chicago, IL 60612-7342.

Cyclic GMP has both stimulatory and inhibitory effects on cardiac calcium current (I_{Ca}) in the presence of isoproterenol (ISO) (Ono & Trautwein, J. Phys. 443:387, 1991). In the present study, the nitric oxide donor SIN-1 similarly stimulated or inhibited I_{Ca} in the presence of 10 nM ISO, depending on the magnitude of the response to ISO. Futhermore, the large stimulatory effect of 100 μM IBMX was reduced by 100 μM SIN-1 (-58$\pm$12%, $p<0.05$ from 100 μM IBMX alone, $n=9$), whereas, the small stimulatory effect of 3 μM IBMX was enhanced by 10 μM SIN-1 (+41$\pm$15%, $p<0.05$ from 3 μM IBMX alone, $n=11$). Pretreatment with the G-kinase inhibitor KT5823 (0.1 μM), which had little effect on the responses to 100 or 3 μM IBMX, inhibited both the stimulatory and inhibitory actions of SIN-1. Thus, the inhibitory effect of 100 μM SIN-1 on the response to 100 μM IBMX was reduced to -21$\pm$2% in the presence of KT ($p<0.05$ from -KT, $n=4$) and the stimulatory effect of 10 μM SIN-1 on the response to 3 μM IBMX was abolished (-11$\pm$5%, $p<0.05$ from -KT, $n=6$). We conclude that nitric oxide is likely to be an important modulator of ß-adrenergic effects on I_{Ca}, and that both the stimulatory and inhibitory effects of nitric oxide are largely mediated by G-kinase-dependent mechanisms.

W-AM-I4

THAPSIGARGIN ACTIVATES CALCIUM CURRENT, YET BLOCKS CYCLIC GMP PRODUCTION IN N1E-115 NEUROBLASTOMA CELLS.
((C. Mathes*, A.A. Alousi, and S.H. Thompson)). Hopkins Marine Station of Stanford University, Pacific Grove, CA 93950 and *IDP in Neurosciences, BRI, UCLA, LA CA 90024.

We studied the calcium dependence of nitric oxide (NO) mediated cGMP production in N1E-115 cells, an excitable cell line derived from mouse sympathetic ganglion. In parallel experiments we measured muscarinic receptor activated cGMP production and changes in $(Ca^{++})_i$, using radioimmunoassay and fura-2 imaging. The muscarinic agonist carbachol (1 mM; 30 sec) stimulated cGMP production 16-fold over baseline. The NO inhibitor L-NMMA (100 μM;1 hour) inhibited cGMP production, while D-NMMA did not, indicating that the process requires NO. The selective ER Ca^{++}-ATPase inhibitor thapsigargin (1 μM; 15 min.) blocked cGMP production by 89% and eliminated calcium release activated by carbachol. Thapsigargin elevated $(Ca^{++})_i$ by 82 ± 35 nM (mean ± SD; n=6) and in nystatin patch experiments thapsigargin activated a calcium current with a peak amplitude of 65 ± 61 pA and current density of 0.22 ± 0.2 pA/pF. Removing external Ca^{++} for 1-2 min. before agonist application reduced cGMP production by 69%, but did not alter calcium release. These data demonstrate that both Ca^{++} release and Ca^{++} entry are imperative for the production of cGMP. [supported by NIH grants NS14519 to S.H.T. and MH10425 to C.M.]

W-AM-I5

AGENTS WHICH BLOCK HEART Cl^- CHANNELS ALSO INHIBIT Ca^{2+} CURRENT REGULATION.

((Kenneth B. Walsh)) University of South Carolina, School of Medicine, Columbia, SC 29208.

We have previously reported that substitution of external Cl^- with I^- not only inhibits the cardiac CFTR/cAMP-dependent protein kinase (PKA)-activated Cl^- current (I_{Cl}), but also decreases the regulation of the L-type calcium current (I_{Ca}) by PKA. Since I^- may act to directly occlude the pore of the Cl^- channel, it was determined whether other Cl^- channel blockers might also inhibit I_{Ca}. Whole-cell I_{Cl} and I_{Ca} were measured in isolated guinea pig ventricular myocytes during stimulation of PKA by forskolin (1 μM) or 8-chlorphenylthio cAMP (200 μM). Diphenylamine-2 carboxylate (DPC) (at 1 mM) caused a large decrease (> 80 %) in both I_{Cl} and the PKA-regulated I_{Ca} (PKA-I_{Ca}). Inhibition of I_{Cl} by DPC occurred in two phases: a relatively fast phase that occurred during the first 30-60 s following drug application, and a slower phase that developed in 2-10 min. Reduction of PKA-I_{Ca} was observed during this slower phase. 5-Nitro-2-(3-phenylpropylamino)-benzoate (NPPB) (50 μM) and anthracene-9-carboxylate (A9C) (500 μM) also strongly reduced both PKA-I_{Ca} and I_{Cl}. In contrast, IAA-94 (50 μM), DNDS (100 μM) or external replacement of Cl^- with Br^- caused no significant decrease in either current. Thus, either DPC, A9C, NPPB and I^- all act in a nonspecific manner to inhibit heart Cl^- and Ca^{2+} channels or there is a relationship between the block of the CFTR Cl^- channel and the PKA-regulation of I_{Ca}.

W-AM-I6

DUAL MODULATION OF CARDIAC INWARDLY-RECTIFYING K^+ CHANNELS BY THE CYCLIC AMP-DEPENDENT PROTEIN KINASE AND PROTEIN PHOSPHATASE.

((S. Koumi, R. E. Ten Eick and J. A. Wasserstrom)) Northwestern University Medical School, Chicago, IL 60611.

We have examined β-adrenergic and cholinergic regulation of the I_{K1} channel in isolated guinea-pig ventricular myocytes using patch-clamp techniques. Isoproterenol (ISO) applied to the bath solution partially inhibited whole-cell I_{K1} after removal of the ISO-induced Cl^- current. Block could be prevented by including a cAMP-dependent protein kinase (PKA) inhibitor in the pipette solution. Bath application of acetylcholine (ACh) could antagonize the inhibition; this effect of ACh could be abolished by preincubating myocytes with pertussis toxin (PTX), suggesting that a muscarinic receptor-coupled, PTX-sensitive G protein, G_i, mediates the ACh-induced antagonism of ISO-induced inhibition of I_{K1}. The suppression of single i_{K1} channels from cell-attached patches induced by bath applied ISO (1 μM) could be inhibited completely by ACh (1-10 μM) applied via the patch pipette. In contrast, bath application of ACh could only partially antagonize the effect of low (e.g., $\leq$ 50 nM) concentrations of ISO but had no effect when 1-10 μM ISO was used. Bath application of the catalytic subunit of PKA to inside-out patches also inhibited i_{K1}, an effect that was antagonized by bath application of alkaline phosphatase, GTPγS or the preactivated G protein subunit $G_{i\alpha}$. When okadaic acid was present in the bath solution, neither GTPγS nor $G_{i\alpha}$ could antagonize the PKA-induced inhibition of i_{K1}. We conclude that I_{K1} can be inhibited by a PKA-mediated phosphorylation; this effect can be antagonized by ACh mainly via a membrane delimited pathway involving activation of G_i which ultimately results in activation of protein phosphatases local to the I_{K1} channel.

W-AM-I7

MECHANISM OF Ca^{2+}-CALMODULIN MODULATION ON THE OLFACTORY CYCLIC NUCLEOTIDE-ACTIVATED CHANNEL.

((T.-Y. Chen, B. Ahamed and K.-W. Yau)) Howard Hughes Medical Institute and Department of Neuroscience, Johns Hopkins University School of Medicine, Baltimore, MD 21205.

We have recently shown that the cyclic nucleotide-activated cation channel in rat olfactory receptor neurons (rOCNC) is subject to a powerful modulation by Ca^{2+}-calmodulin (CaM); namely, with CaM bound, the channel's apparent affinity for cyclic nucleotide is substantially reduced, as indicated by the half-activating cyclic nucleotide concentration ($K_{\frac{1}{2}}$) increasing by ca. 10 fold for the expressed channel and ca. 20 fold for the native channel (Chen and Yau, Soc Neurosci Abstr 19: 13, 1993). We report here experiments to examine the molecular mechanism for this modulation, employing mutagenesis and the HEK 293 cell expression system. Using chimeric channels composed partly of rOCNC and partly of the human rod cyclic nucleotide-activated channel subunit 1 (hRCNC1, which does not show any CaM effect), we have identified the cytoplasmic N-terminal segment of rOCNC to be necessary for the CaM action. Using deletion mutants of rOCNC, we have further identified a small domain on this N-terminal segment that, when deleted, results in a mutant channel with a $K_{\frac{1}{2}}$ increase by ca. 10 fold compared to wild-type and also becoming unresponsive to CaM. One interpretation of the results is that this domain is an important determinant for tight cyclic nucleotide binding, but its influence is removed (perhaps by steric hindrance) when CaM presumably binds to the vicinity.

W-AM-I8

DOES CALCINEURIN MEDIATE Ca^{2+} DEPENDENT INACTIVATION OF L-TYPE CALCIUM CURRENTS IN GH_3 CELLS?

((R.G. Victor, E. Marban, and B. O'Rourke)) Johns Hopkins Univ, Baltimore, MD 21205 and UT Southwestern Med Ctr, Dallas, TX 75235

Channel dephosphorylation by calcineurin, the Ca^{2+}-calmodulin dependent phosphatase (2B), has been proposed to mediate Ca^{2+}-dependent inactivation of L-type Ca^{2+} currents ($I_{Ca,L}$) in GH_3 cells. The novel immunosuppressive drugs Cyclosporin A and FK506 are specific inhibitors of calcineurin thus providing new opportunities to test this hypothesis. Using whole cell patch-clamp, $[Ca^{2+}]_i$ was rapidly increased with flash photolysis of caged Ca^{2+} (5mM DM-nitrophen). Using a 2-pulse protocol with varying prepulse voltages and a constant test pulse to +20mV (V_{hold} = -40mV), the I-V relation displayed a U-shaped curve with 25mM Ca^{2+} as the charge carrier: maximal inactivation occurred with a prepulse to +20mV and partial recovery from inactivation was evident at +60mV. Under control conditions (n=6), photorelease of Ca^{2+} decreased $I_{Ca,L}$ from 200±76 to 129±53 pA (mean±SE, $p<0.05$), increased inactivation from 46±10 to 66±11% ($p<0.05$), and increased recovery from inactivation from 11±3 to 28±7% ($p<0.05$). These robust responses were unaffected by cyclosporin A (2μM, 24h incubation,n=5), FK506 (1μM pipette solution, n=5), or fenvalerate (2μM, 30min incubation, n=5), another potent calcineurin inhibitor. Thus, our experiments to date failed to provide evidence that calcineurin regulates Ca^{2+} channel inactivation in GH_3 cells.

W-AM-I9

THE G PROTEIN G_q OPENS TWO K^+ CHANNELS VIA A MEMBRANE-DELIMITED PATHWAY.

((M.A. Harrington, S. Gutowski and F. Belardetti)) Dept. Pharmacol., U.T. Southwestern, Dallas, TX 75235.

The highly homologous, pertussis toxin (PTX)-insensitive G proteins G_q and G_{11} couple the bradykinin (BK) receptor to phosphoinositol-specific phospholipase C (PI-PLC). In neuroblastoma x glioma (NG108-15) cells $G_{q/11}$ also couple BK receptors to the activation of a K^+ current ($I_{K,BK}$). This action was thought to be due exclusively to PI-PLC-dependent IP_3 release and subsequent increase in $[Ca^{2+}]_i$. Using whole-cell patch clamp recordings we now demonstrate that there is a component of the $I_{K,BK}$ which functions even under conditions in which the IP_3/Ca^{2+} pathway is disrupted. In cell-free patches, we have identified two small-conductance K^+ channels which open in response to either BK or GTPγS, and show that both opening responses are blocked by an anti-$G_{q/11}$ IgG. These results provide the first indication that $G_{q/11}$ mediate regulation of K^+ channels via a membrane-delimited pathway.

W-AM-J1

THE FIDELITY OF T7 DNA POLYMERASE AND HIV-REVERSE TRANSCRIPTASE IS DETERMINED BY AN INDUCED FIT MECHANISM. (S.G. Edwards and K.A. Johnson) Dept. of Molecular & Cell Biology, 106 Althouse Laboratory, Pennsylvania State University, University Park, PA 16802 (Sponsored by R. Zauhar).

In this report we show that both T7 DNA polymerase and HIV- reverse transcriptase(RT) check not only the correct Watson-Crick geometry of the incoming base but also the bases already incorporated in the duplex region of the primer-template. Primer-templates with mismatches at various positions(n-1, n-2 to n-7) from the 3'-OH end were used as substrates to examine the rate of correct nucleotide incorporation in single turnover experiments. The single turnover experiments provided estimates of the K_d for dTTP, the rate of the incorporation and DNA binding as a function of the distance of the mismatched base-pair from the 3'-OH terminus. This presteady state kinetic analysis reveals that mismatches at the n-1, -2 and -3 positions reduce the rate of continued correct polymerization and weakens the binding of the incoming correct nucleotide. Mismatches at the n-4, -5 or beyond have little effect on the rate of continued polymerization and nucleotide binding. These data serve to map out the binding pocket as it relates to the ability of the polymerase to undergo a conformational change responsible for Watson-Crick base-pair recognition. We argue that the fidelity of DNA polymerization is established globally by an induced fit mechanism and is operative for at least two DNA polymerases (Supported by NIH grant GM 44613).

W-AM-J2

ELUCIDATION OF CONFORMATIONAL CHANGES DURING DNA POLYMERIZATION CATALYZED BY HIV-1 RT ((Ahamindra Jain and Kenneth A. Johnson*)), Department of Molecular and Cellular Biology, The Pennsylvania State University, University Park, PA 16802

DNA polymerization catalyzed by HIV-1 Reverse Transcriptase (RT) involves a rate-limiting conformational change, which follows binding of primer/template and nucleotide substrates (Kati, W.M. *et al.* 1992. *J. Biol. Chem.* 267: 25988-25997). Binding of the DNA substrate alone to RT results in a decrease in protein fluorescence, suggesting that the orientations of some amino acid side chains are affected during this event. Identification of the specific region(s) of RT participating in these processes may suggest novel targets for the design of anti-viral agents that inhibit these key steps in replication.

Pre-steady state stopped flow and rapid chemical quench experiments will be described that quantitatively address the nature of these conformational changes. In addition to studies with random sequence primer/templates, results from experiments with DNAs bearing fluorescence probes at specified locations in the primer and template strands, blunt-ended substrates, and intrinsically bent DNAs will be presented. These data will also be considered in light of the recently published co-crystal structure of HIV-1 RT bound to primer/template (Jacobo-Molina, A. *et al.* 1993. *Proc. Natl. Acad. Sci.* 90: 6320-6324).

Supported by NIH Grant 44613-03

W-AM-J3

DISPLACEMENT OF THE E. COLI CYCLIC AMP RECEPTOR FROM THE LACTOSE OPERATOR BY LAC REPRESSOR ((M. G. Fried[1] and J. M. Hudson[2])) [1]Department of Biochemistry, Pennsylvania State University College of Medicine, Hershey, PA 17033. [2]Department of Cell Biology, M.D. Anderson Cancer Center, Houston, TX 77030

The lactose repressor and the cyclic AMP receptor protein (CAP) regulate the transcriptional activity of the E. coli lactose operon. In the lactose promoter-operator region, the principal repressor binding site (operator 1), overlaps with a high affinity CAP binding site (CAP site 2). When these proteins bind individually, they occupy the same face of the DNA. Thus, binding competition resulting in the displacement of one or both proteins is expected to occur. We have found that lactose repressor is capable of displacing CAP from the operator 1-CAP site 2 region. The affinity of CAP for the sites to which it is displaced is ~10^{-5} times that for CAP site 2. Because of this, the displacement of CAP from CAP site 2 to non-specific DNA sequences should change the apparent affinity of lactose repressor for operator 1 by a factor of ~10^{-5}. However, we find that CAP displacement has nearly no observable effect on the apparent affinity of repressor for operator 1. A possible resolution of this discrepancy is provided by the observation that when displaced, CAP occupies discrete sites adjacent to those bound by repressor, even though its intrinsic affinity for those sites is not significantly greater than that for average genomic sequences. This suggests that interactions between CAP and repressor compensate for the loss of favorable protein-DNA interactions that must occur when CAP is displaced from CAP site 2 to non-specific sites. Supported by NSF grant DMB-91-96154.

W-AM-J4

RATES OF *LAC* REPRESSOR-MEDIATED LOOP FORMATION AND BREAKDOWN MEASURED IN SINGLE DNA MOLECULES. ((L. Finzi*[1] and J. Gelles*)) *Dept. of Biochemistry and Ctr. for Complex Systems, Brandeis Univ., Waltham, MA 02254; [1]Dept. of Biology, Univ. of Milan, Milan, Italy.

Protein-mediated DNA looping is an essential feature of many transcriptional regulation mechanisms. Tetrameric *E. coli lac* repressor protein induces DNA loop formation both *in vivo* and *in vitro*. We have measured the rates of formation and breakdown of such loops using the tethered particle motion (TPM) method [c.f. Schafer *et al.* (1991) *Nature* 352, 444-448], which allows quantitative, real-time measurement of the dynamics of individual DNA molecules. A 1.3 kbp DNA containing two primary *lac* operators separated by 301 bp was labelled with digoxigenin at one end and biotin at the other. The DNA was used to tether avidin-conjugated 0.2 μm-diameter polystyrene particles to an anti-digoxigenin-coated glass surface under conditions in which most tethered particles were attached to a single DNA molecule. The spatial extent of particle Brownian motion (r) was measured to ca. ±10 nm precision at 0.5 Hz using video light microscopy and digital image processing. Without repressor, r is ~75 nm. With 1.0×10^{-9} M repressor, the particles exhibit stochastic fluctuations between two discrete states with r ~45 nm and ~75 nm. A variety of experimental results suggest that these states correspond, respectively, to looped and unlooped configurations of the DNA. The unlooped state lifetimes have a multiphasic distribution, consistent with models in which this state consists of several chemical species. The looped state lifetimes are exponentially distributed with an apparent first order unlooping rate constant of 0.02 s^{-1} (22°), demonstrating that loop strain does not substantially increase the repressor-operator dissociation rate and excluding rapid unlooping by repressor tetramer dissociation. The TPM technique is a powerful, generally applicable approach to analyzing the kinetics of complex protein-DNA interactions.

W-AM-J5

THERMODYNAMIC LINKAGE BETWEEN LIGAND BINDING AND DIMERIZATION OF THE REPRESSOR OF BIOTIN BIOSYNTHESIS ((Edward Eisenstein* and Dorothy Beckett#)) Department of Chemistry and Biochemistry, University of Maryland Baltimore County#*, Baltimore, MD 21228 and CARB* (Spon. by C. Fenselau)

The repressor of biotin biosynthesis binds to the biotin operator, a 40 base pair inverted palindrome, to repress transcription of the biotin biosynthetic genes. Sequence specific DNA binding of BirA is allosterically coupled to binding of the effector molecule, bio-5'-AMP. The DNA binding mechanism involves cooperative association of two holorepressor monomers with the two operator half sites. One structural locus of the cooperativity may lie in a protein-protein interface that forms between adjacently bound monomers. In an effort to examine the relationship between DNA binding and protein assembly in this system, we have determined the assembly state of the protein alone and in the presence of ligands using equilibrium sedimentation techniques. Experiments were performed on a Beckman ModelE Analytical Ultracentrifuge. Results of these measurements indicate that the aporepressor and the repressor-biotin complex are monomeric at protein concentrations up to 50μM. The binary complex of BirA with bio-5'-AMP and the ternary complex of BirA with bio-5'-AMP and a double stranded half operator oligomer are, however, best described as a mixture of monomers and dimers and a single dimeric species, respectively. These results indicate that binding of both Bio-5'-AMP and DNA to BirA are positively coupled to dimerization of the repressor and support the notion that the structural locus for cooperative DNA binding in this system lies, in part, at a protein-protein interface formed between adjacently bound monomers.

W-AM-J6

PEPTIDE MAPPING A NUCLEIC ACID BINDING SITE: MASS SPECTROMETRY, PHOTOAFFINITY LABELING AND TRANSCRIPTION TERMINATION FACTOR RHO. ((Stephen Swenson*, Ole N. Jensen‡, Douglas F. Barofsky† and Steven E. Seifried*)). *Department of Biochemistry and Biophysics, University of Hawaii, Honolulu, HI 96822 ‡Department of Biochemistry and Biophysics, Oregon State University, Corvallis, OR 97331 †Department of Agricultural Chemistry, Oregon State University, Corvallis, OR 97331

The development and combination of two techniques presents the opportunity to rapidly determine which amino acid residues of a protein constitute nucleotide or nucleic acid binding sites. Others have shown the naturally occurring chromophore 4-thiouracil to form a short-lived thione radical when irradiated with 335 nm light, a wavelength away from other biological absorbances. The excited state will insert into carbon-carbon or carbon-nitrogen bonds forming a stable photoadduct with neighboring peptides. If a charge transfer reaction does not occur within the excited state lifetime of microseconds the photoprobe will relax to the initial species, avoiding non-productive photoproducts. In our experiments 4-Thiouracil-containing nucleotides are bound to the nucleotide triphosphate or polynucleotide binding sites of *E. coli* transcription termination factor rho and irradiated. The photolabeled protein is digested with trypsin and subjected to microbore liquid chromatography/electrospray ionization mass spectrometry that provides on-line identification of chromatographically separated tryptic fragments by mass spectrometric molecular weight determination. Furthermore, peptides can be sequenced by tandem mass spectrometry as they elute off the LC column. In this manner the amino acids that are adducted to the 4-thiouracil are identified.

W-AM-J7

FLUORESCENCE ANALYSIS OF THE TRANSCRIPTIONAL ACTIVATION DOMAIN OF THE HERPESVIRUS PROTEIN VP16 REVEALS A HIGHLY FLEXIBLE STRUCTURE. ((Fan Shen*, Steven J. Triezenberg*, Denise Porter#, Jay R. Knutson#, and Preston Hensley+)) *Dept. of Biochemistry, Michigan State University, East Lansing MI 48824-1319, #NHLBI, LCB, NIH, Bethesda MD 20892, and +Dept. of Macromolecular Sciences, SmithKline Beecham, King of Prussia PA 19406-0939.

VP16, a virion protein of herpes simplex virus, specifically and potently activates transcription of viral immediate early genes. The transcriptional activation function has been mapped to the C-terminal 78 amino acids (residues 413-490). Extensive mutational analysis has shown that this function can be diminished or abolished by subtle amino acid substitutions in this domain. Biochemical analyses suggest that VP16 activates transcription by interacting with TFIID, TFIIB, or other components of the basal transcriptional machinery through contact with the activation domain. However, little is known about the structure of the domain or the mechanism by which it interacts with these proteins. Here, we describe a fluorescence analysis employing chimeric proteins comprising the DNA-binding domain of GAL4 (1-147) fused to the activation domain of VP16 (413-490 or subdomains thereof). Trp36 of GAL4 was replaced by Val and Trp residues were substituted for Phe at either 442 or 473 of VP16, with only modest effects on activity, thus obtaining unique fluorescence probes at two positions in the activation domain. The results of dynamic quenching, DAS, and time-resolved anisotropy studies show that the Trp residues at either position have very similar fluorescence properties, are highly mobile and are very solvent exposed. These results are not predicted by mutational studies, which suggest that the activation function requires some specific structure. These data are compatible with published CD and NMR analyses of peptides containing the VP16 activation domain. Together, these data suggest that a significant structural transition in the activation domain must accompany interaction of VP16 with target protein(s) in the basal transcription machinery.

W-AM-J8

AN *IN VITRO* MODEL OF CARDIAC MYOCYTE HYPERTROPHY DISPLAYS DOWN-REGULATION OF THE MESSENGER RNAs (MRNAs) ENCODING CA^{2+}-CYCLING PROTEINS. ((S.A. Fisher, M. Absher, M. Periasamy, N.R. Alpert, and A.S. Rovner)) Department of Molecular Physiology and Biophysics, University of Vermont College of Medicine, Burlington, VT 05405.

The expression of mRNAs encoding the sarcoplasmic reticular proteins involved in Ca^{2+} cycling decrease both in animal models of pressure overload hypertrophy and in human heart failure. To test the hypothesis that increased levels of circulating catecholamines present in these conditions mediate such changes in gene expression, we have implemented a cell culture model of cardiac myocyte hypertrophy. Rat neonatal cardiocytes were isolated by serial enzyme digestion, and cultured in the presence or absence of 2 μM norepinephrine (NE) in a defined, serum-free medium. In some experiments, thyroid hormone (T3) was also included in the medium. Hypertrophy was assessed by measuring the amount of protein per cell, and the levels of the mRNA for calsequestrin (CSQ), phospholamban (PL) and the cardiac/slow muscle sarco-endoplasmic reticulum Ca^{2+}-ATPase isoform (SERCA2) were assessed by northern blotting and normalization to the levels of glyceraldehyde phosphate dehydrogenase (GAPDH) mRNA. NE caused a substantial increase in the amount of protein per cell irrespective of T3 status. However, in T3-containing cultures, treatment with NE produced a 30-50% decrease in the steady-state levels of SERCA 2, CSQ and PL mRNA. This result indicates that NE may modulate T3-sensitive gene expression in cardiac muscle cells, and suggests a mechanism for the down-regulation of Ca^{2+} cycling proteins in heart failure. (Supported by NIH P01 HL28001-11).

PROTEIN FOLDING: RECOGNITION OF SUBMOLECULAR DOMAINS

W-PM-Sym-1

PROTEIN MOTIFS AND FOLDING RECOGNITION. ((J.M. Thornton[1], C.M. Orengo[1], D.T. Jones[1,2], W.R. Taylor[2])) [1]Biomolecular Structure and Modelling Unit, Biochemistry and Molecular Biology Dept., University College London. Gower Street, London WC1E 6BT, UK. [2]National Institute for Medical Research, The Ridgeway, Mill Hill, London NW7 1AA, UK.

When a new protein structure is solved, it is becoming increasingly common to find that this structure closely resembles another entry in the Protein Structure Databank, (PDB) despite a lack of sequence or functional similarity. We have known for some time that there is a limited number of secondary and supersecondary motifs (eg. $\beta\beta$-hairpin, Greek Key, $\beta\alpha\beta$ unit) and it is now apparent that this translates into a limited number of protein folds. We have systematically identified structural similarities in the PDB and classified the folds into families (1). In the $\beta+\alpha$ family of structures we find that two motifs (the split $\beta\alpha\beta$ unit and the $\beta\beta\beta\alpha$ meander) are very common (2). In the universe of proteins, the structures segregate into 3 groups (all α, all β and $\alpha\beta$), but some topologies recur much more frequently than expected (eg. the TIM barrels). We have been able to use the current growth in the database, combined with a knowledge of which folds recur, to estimate the total number of folds. Furthermore, the fold library we derive, provides the target structures for fold recognition from amino acid sequence, using the optimal sequence threading algorithm combined with empirical potentials (3). Recent results will be described.

1. Orengo C.M. et. al. (1993) Protein Eng. 6 485-500
2. Orengo C.M. et. al. (1993) Structure. 1 105-120
3. Jones D.T. et. al. (1992) Nature. 358 86-89

W-PM-Sym-2

THE SLOW EXCHANGE CORE AS THE PROTEIN FOLDING CORE. **((Clare Woodward)) Dept. of Biochemistry, University of Minnesota, St. Paul, MN 55108.**

The slow exchange core of a native protein contains the last 3-8 peptide NH hydrogens to undergo isotope exchange with solvent. It consists of segments of secondary structure packed by hydrophobic groups. The slow exchange core is highly correlated with sequences containing NH groups that are protected first during folding, and with those that are slowly exchanging in partially folded proteins. The correlation of the slow exchange core to the folding core suggests an insight into the central logic of protein structure and folding (Kim et al., *Biochemistry* 32, 9600-9608; Woodward, Cur. Op. Str. Biol. in press). Structure implies process; in this case, native state dynamic structure reflects initial events in folding, or, rigid native structure predicts function in folding. The region that is least flexible by H-exchange criteria apparently contains the noncontiguous segments involved in early folding interactions. The proposal is that the slow exchange core is *the* hydrophobic core, or essential tertiary kernel, containing the sequences encoding the fold. (Large proteins may have more than one.) Peptides with sequences corresponding to the core are expected to have a native-like fold. Partially folded proteins (molten globules, A states) are expected to be collapsed in the region of the slow exchange core. These points are illustrated by the folding behavior of BPTI having only one intact disulfide bond, 14-38.

W-PM-Sym-3

PROTEIN FOLDING: DRIVING FORCES AND THE LEVINTHAL PARADOX. ((Ken A. Dill, Kai Yue, and Klaus Fiebig)) University of California, San Francisco, CA 94143-1204

What forces drive the compactness, the symmetries and internal architectures, and the uniqueness, cooperativity, and folding kinetics of globular proteins? One view holds that proteins are folded by hydrogen bonding and helical tendencies of peptide bonds. We have explored an alternative view that the properties of globular proteins are mainly encoded in their sequences of hydrophobic and polar amino acids. We have recently found that some tertiary structural symmetries ("designable sequences") arise from sequences of nonpolar and polar amino acids that can fold to the fewest incorrect alternatives. The Levinthal paradox is the question of how a protein can find its unique native conformation without endless searching of its enormous conformational space. We believe proteins fold as "hydrophobic zippers."

W-PM-Sym-4

PROTEINS IN PIECES. ((J. CAREY)) Chemistry Dept., Princeton University, Princeton NJ 08544-1009.

Proteolytic dissection of native *trp* repressor and horse heart cytochrome c has been used to infer some of the steps in the folding pathways of the intact proteins. For both proteins, small fragments are capable of undergoing spontaneous noncovalent association to form subdomains with native-like secondary and/or tertiary structural features, suggesting that dissection/reassembly may be a general method to gain insight into the structures of folding intermediates. The importance of this approach is its simplicity and potential applicability to studying the folding pathways of a wide range of proteins. The proteases report on the structure and dynamics of the native state, circumventing the need for prior knowledge of the structures of folding intermediates. The observation that small fragments of proteins can associate noncovalently suggests that protein folding can be viewed as an intramolecular "recognition" process. The results imply that substantial information about protein structure and folding is encoded at the level of subdomains, and that chain connectivity has only a minor role in determining the fold.